

FEASIBILITY OF SMALL-SCALE URBAN WIND ENERGY GENERATION

by

Mark A. Moriarty

B.S. in Civil Engineering, Texas A&M University, 2008

Submitted to the Graduate Faculty of

Swanson School of Engineering in partial fulfillment

of the requirements for the degree of

Master of Science

University of Pittsburgh

2009

UNIVERSITY OF PITTSBURGH

SWANSON SCHOOL OF ENGINEERING

This thesis was presented

by

Mark Moriarty

It was defended on

July 31, 2009

and approved by

Amy Landis, Assistant Professor, Departmental of Civil and Environmental Engineering

Lisa Weiland, Assistant Professor, Departmental of Mechanical Engineering and Materials
Science

Thesis Advisor: Kent Harries, Associate Professor, Departmental of Civil and Environmental
Engineering

Copyright © by Mark Moriarty

2009

FEASIBILITY OF SMALL-SCALE URBAN WIND ENERGY GENERATION

Mark Moriarty, M.S.

University of Pittsburgh, 2009

This study examines the environmental impacts and the viability of placement in an urban environment of a small-scale wind energy prototype known as an Aeroelastic Energy Harvester (AEH). Using Life Cycle Assessment (LCA), the prototype was modeled using SimaPro v.7 in order to create a baseline. Results include information on the energy required to produce and manufacture the AEH, as well as environmental impacts associated with production. Alternative materials for the frame of the AEH such as recycled aluminum instead of virgin aluminum or plywood instead of acrylic sheets were also studied to determine their impacts relative to the prototype's current materials. A decision matrix was created to 'rank' these materials based on a number of categories, including weight, durability, and energy consumption. Two alternative frame models were created and their impacts relative to the prototype were presented.

The second portion of the study proposes a method to transform open field wind data into wind speeds in a built-up urban environment using characteristics of localized wind flows in urban areas including surface roughness, elevation and concentrator effects. An example of wind speeds at selected buildings in Pittsburgh, PA is presented. Using current data of the prototype AEH outputs, a range of outputs were calculated for each of four selected buildings. The current results suggest the AEH will be suitable for applications such as wireless sensors and providing 'trickle' charging capabilities for battery operated systems. As development continues and output increases, the AEH may be able to play a bigger role in supplying on-site electricity.

TABLE OF CONTENTS

NOMENCLATURE.....	XI
ACKNOWLEDGEMENTS	XIII
1.0 INTRODUCTION.....	1
1.1 MOTIVATION	2
1.1.1 Wind Power Class.....	4
1.2 WIND ENERGY GENERATING DEVICES.....	5
1.2.1 Horizontal Axis Wind Turbine.....	5
1.2.2 Vertical Axis Wind Turbine	7
1.2.3 Aeroelastic Energy Harvester.....	7
2.0 LITERATURE REVIEW.....	15
2.1 LIFE CYCLE ASSESSMENT.....	15
2.2 WIND ENERGY GENERATION ENVIRONMENTAL IMPACTS.....	17
2.2.1 Large-Scale Wind Turbines.....	17
2.2.2 Small-Scale Wind Turbines	20
2.3 WIND ENVIRONMENT	24
2.3.1 Open Field Flow.....	25
2.3.2 Flow in the Built Environment.....	26
2.3.2.1 Urban Canopy Model	30

2.4	ISSUES AFFECTING SMALL-SCALE WIND TURBINE SITING	31
2.4.1	Bluff bodies and concentrator effects	32
2.4.2	Turbulence and Flow Separation.....	33
2.4.3	Wind-induced Pressure.....	35
2.4.4	Wind Power Density.....	37
2.4.5	Current Turbine Performance in Urban Areas.....	37
2.5	GENERAL CONCLUSIONS FROM LITERATURE REVIEW.....	38
3.0	LIFE CYCLE ASSESSMENT OF AEH.....	46
3.1	GOAL AND SCOPE.....	47
3.1.1	Objective and Scope	47
3.1.2	Functional Unit	47
3.2	LIFE CYCLE INVENTORY.....	48
3.2.1	Current AEH Materials	48
3.2.2	System Boundaries	48
3.2.3	Alternative Material Options	50
3.3	RESULTS OF LIFE CYCLE IMPACT ASSESSMENT.....	51
3.3.1	Energy Consumption.....	51
3.3.2	Environmental Impacts and Energy Payback Period.....	52
3.3.3	Comparison with Other Energy Methods.....	53
3.4	SENSITIVITY ANALYSIS	54
3.4.1	Energy Consumption.....	54
3.4.2	Environmental Impacts and Energy Payback Period.....	55
3.4.3	Comparison with Other Energy Methods.....	57

3.5	DISCUSSION OF RESULTS	57
4.0	LOCAL WIND ENERGY GENERATION IN AN URBAN ENVIRONMENT .	64
4.1	WIND ENERGY POTENTIAL IN PENNSYLVANIA	64
4.2	PITTSBURGH DATA COLLECTION AND ANALYSIS.....	65
4.3	PITTSBURGH WIND ENVIRONMENT	66
4.3.1	Step 1: Open Field Wind Profile	66
4.3.2	Step 2: Change of roughness into urban location.....	67
4.3.3	Step 3: Flow around buildings/concentrator effects.....	69
4.3.4	Step 4: Apply current AEH output results.....	71
4.4	POTENTIAL USE OF AEH IN COMMERCIAL BUILDINGS.....	73
4.5	CONCLUSIONS ON PITTSBURGH WIND ENVIRONMENT	74
5.0	CONCLUSIONS AND FUTURE RESEARCH DIRECTIONS.....	90
5.1	FUTURE RESEARCH DIRECTIONS	92
	BIBLIOGRAPHY	94

LIST OF TABLES

Table 1.1: Wind Power Classes (U.S. Department of Energy, 2009).....	10
Table 1.2: AEH from Humdingerwind.com (Humdinger, 2009)	10
Table 2.1: Small-Scale HAWTs	40
Table 2.2: Wind Turbine Impacts and Savings over 15 year lifetime (Allen et al., 2008).....	40
Table 3.1: Impacts due to AEH production: current version and alternatives.....	59
Table 3.2: Decision Matrix for alternative material options.....	60
Table 3.3: Required AEH Outputs for Selected Payback Periods	60
Table 4.1: Wind Data Summary at 10 m height	77
Table 4.2: Summary of wind speed values at roof levels	78
Table 4.3: Summary of k and n values in power curve creation.....	78
Table 4.4: Wind speeds (m/s) used in AEH power calculations.....	79
Table 4.5: Electricity outputs for a single AEH on Pittsburgh Hilton roof	79
Table 4.6: Electricity outputs for a single AEH on Westinghouse Tower roof.....	80
Table 4.7: Electricity outputs for a single AEH on Westinghouse Tower recessed area	80
Table 4.8: Electricity outputs for a single AEH on U.S. Steel Building roof.....	81
Table 4.9: Electricity outputs for a single AEH on FHL Bank Building roof.....	81

LIST OF FIGURES

Figure 1.1: US Electricity Net Generation, 2008.....	11
Figure 1.2: Cumulative Installed US and World Wind Energy Capacity (GW)	11
Figure 1.3: US Wind Power Class Map (US Department of Energy, 2009)	12
Figure 1.4: Examples of Horizontal Axis Wind Turbines (HAWT)	13
Figure 1.5: Examples of Vertical Axis Wind Turbines (VAWT).....	14
Figure 1.6: Current Progress on AEH at University of Pittsburgh	14
Figure 2.1: Schematic of Wind Profiles (Mertens, 2003).....	41
Figure 2.2: Flow characteristics inside RS (adapted from Grimmond and Oke, 1999).....	41
Figure 2.3: Setup and selected results from Ricciardelli and Polimeno (2006).....	42
Figure 2.4: Results from Skote et al. (2005).....	43
Figure 2.5: Velocity Profile through Canopy ($x/b=0$ to $x/b = 18$) (Coceal, 2003)	43
Figure 2.6: Prism Figures from Kim et al. (2003)	44
Figure 2.7: Wind pressure coefficients for a gable/hip roof system (ASCE 7-05).....	45
Figure 3.1: AEH flowchart (dashed boxes are outside the system boundaries)	61
Figure 3.2: Percentage share of energy consumption of primary AEH materials	61
Figure 3.3: Normalized results for energy consumption and GWP.....	62
Figure 3.4: Normalized Impacts of Prototype, Decision Matrix, and Minimum Environmental Impact options.....	63

Figure 4.1: Pennsylvania Wind Power Map (US Department of Energy, 2009).....	82
Figure 4.2: Pittsburgh Region showing downtown (center right) and airport (left)	82
Figure 4.3: Wind Characteristics for Pittsburgh, PA, 2005-2008.....	83
Figure 4.4: Views of Pittsburgh, PA.....	84
Figure 4.5: Perimeter Buildings for Pittsburgh study	85
Figure 4.6: Interior Buildings for Pittsburgh Study	86
Figure 4.7: Potential AEH Power Curves	87
Figure 4.8: Wind Characteristics for AEH Operating Range 236° to 304°	88
Figure 4.9: Hourly Electric loads for 250,000 ft ² Chicago office building (US EPA)	89

NOMENCLATURE

AEH:	Aeroelastic Energy Harvester
BAWT:	Building Augmented Wind Turbine
C:	Pressure Coefficient
CFD:	Computational Fluid Dynamics
CL:	Canopy Layer
CO ₂ :	Carbon Dioxide
CO _{2eq} :	Carbon Dioxide Equivalent
d _o :	Displacement Height
EFLH:	Equivalent Full-Load Hours
GHG:	Greenhouse Gas
GWh:	Gigawatt-hour
GWP:	Global Warming Potential
h:	Height of Roughness Sublayer
HAWT:	Horizontal Axis Wind Turbine
ISO:	International Organization for Standardization
k:	von Karman constant
kWh:	kilowatt-hour
LCA:	Life Cycle Assessment

LCI:	Life Cycle Inventory
LCIA:	Life Cycle Impact Assessment
p:	Design Wind Pressure
q:	Dynamic Wind Pressure
RES:	Renewable Energy Sources
RS:	Roughness Sublayer
TKE:	Turbulent Kinetic Energy
TRACI:	Tool for the Reduction and Assessment of Chemical and Other Environmental Impacts
u:	Wind Speed
u*:	Friction or Shear Velocity
VAWT:	Vertical Axis Wind Turbine
WPD:	Wind Power Density
x:	Horizontal Distance from Change in Roughness
z:	Elevation from Ground Level
z ₀ :	Roughness Length
α:	Coefficient in Power Law
δ(z ₀):	Depth of Surface Layer based on z ₀
ρ:	Air Density

ACKNOWLEDGEMENTS

To Dr. Kent Harries: Thank you for your guidance and support throughout this process. Your assistance and advice helped me overcome the many challenges of writing this thesis.

To Dr. Amy Landis: Thank you for the encouragement and assistance you have provided. It has been instrumental in achieving my research goals, and in my other academic studies.

To the Sustainability and Green Design faculty and students: Thank you for the encouragement you have provided during my time here. Your energy, knowledge, and support more than confirmed that the University of Pittsburgh for my graduate studies was the correct place for me.

To my wife, Michelle: Your unwavering support, patience, and love throughout my graduate career have been invaluable. You were always there to push me whenever I faltered and I love you even more for that.

1.0 INTRODUCTION

In this work, two primary topics were studied. First, the environmental impacts of a new prototype small-scale wind energy generator known as an Aeroelastic Energy Harvester (AEH) were investigated. Studying different material combination options for the AEH prototype provided a comparison with baseline results. Second, the potential for local wind energy generation in an urban setting was studied. While the majority of wind energy in the US and the world comes from large-scale production in open fields, taking advantage of the local wind effects in a built environment has the potential to increase on-site electricity generation capacity.

The first part of the study takes a Life Cycle Assessment (LCA) approach to investigate the feasibility and environmental impacts of a novel small-scale wind energy electricity generating device – the “AEH”. LCA is the study of a product, process, or industry, taking into account all phases of their life, from raw material extraction and acquisition to eventual decommissioning and disposal. Products, processes, and industries are complex, consisting of many stages, with multiple entities working independently to produce a final product. More often than not, each entity will focus on their primary task while ignoring the impacts of the other phases. For example, a company that produces doors to sell to an auto manufacturer is often only worried about the direct impacts of producing the doors. They will not necessarily focus on how the door will eventually be disposed of or recycled, or how the materials for their door were

extracted, etc. LCA promulgates a holistic view of the impacts of the door's manufacture, use, and end-of-life. For the LCA conducted in the present study, two questions have been posed and answered: 1) Using LCA, what are the life cycle environmental impacts of manufacturing the AEH prototype and how does altering some of its primary components affect these impacts? 2) How do the environmental impacts of the AEH compare to its competition, such as solar power or other small-scale wind turbines?

While average wind speeds in urban environments are typically lower than wind speeds in rural areas, there is still potential for wind energy generation in urban districts. The second portion of the research addresses the steps that are required to use readily available data, such as airport wind speed and direction, to determine wind energy generation potential in an urban environment. By doing so, the viability of small-scale wind energy generation and issues associated with physically siting such projects are investigated. A detailed study of how wind moves from a 'free field' into an urban environment as well as the local characteristics of wind flow (accelerations, turbulence, pressures, etc) as it interacts with buildings (bluff bodies) and through building canyons is presented.

1.1 MOTIVATION

The United States uses more electricity than any other country in the world. The US consumed 4.11 trillion kilowatt hours (kWh) of electricity in 2008 (Energy Information Administration, 2009). China, the world's second largest consumer of electricity, consumed only 2.83 trillion kWh in 2006, which is the most recent data available. With populations of approximately 300

million and 1.3 billion, per capita electricity use in the US and China are 13,700 kWh and 2,200 kWh respectively.

The US relies heavily on fossil fuels, such as coal and natural gas, to meet its electricity demands. Over ninety percent of the electricity generated in the US comes from such non-renewable energy sources (Figure 1.1), with the remaining provided by renewable energy sources (RES). While there is debate surrounding classifying nuclear as a RES, in this study, renewable energy will refer to only hydroelectric, wood, biofuels, waste, geothermal, wind, and solar power (Energy Information Administration, 2007).

While RES are only a fraction of the total energy mix, wind energy development in the US has been on the rise, increasing capacity at an average annual rate of 32% over the past five years ending in 2008 (GWEC, 2008). In 2008, new wind energy projects accounted for 42% of all the added electricity generation capacity in the United States. The total installed wind power capacity in the US now stands at 25.2 GW, which is just over 1% of the nation's total capacity (GWEC, 2008). Figure 1.2 shows the rapid increase of installed wind energy capacity in the US and internationally. While the US has not always been at the forefront of the wind energy movement, its percentage of worldwide wind energy capacity has increased from 14% to 21% in the last five years. In 2008, the US held the top market spot in both new capacity and passed Germany to claim the top position in terms of total capacity, proving the United States' leadership in this expanding field (GWEC, 2008).

1.1.1 Wind Power Class

Wind as a potential energy source is described by its Wind Power Classification. This system consists of seven distinct levels of resource potential, ranging from Poor (class 1) to Superb (class 7). Each stratum is defined by its Wind Power Density (WPD), which is a measure of energy available to be converted by a turbine (see Table 1.1). Wind Power Density will be discussed in more detail in a later section of this thesis.

Geographically, most of the US consists of class 1 through 4 sites, with classes 5 through 7 being located along coastlines (Figure 1.3). For large-scale wind projects, selecting a site with a class 4 rating or greater will generally provide a suitable location. As Figure 1.3 illustrates, the amount of land in the US rated as being class 4 or higher is relatively small. Additionally, with the exception of coastal or off-shore generation (which has issues of its own), the majority of suitable locations for large-scale projects (such as the high plains) do not correspond with locations of the highest energy demand. Thus, further reliance and upgrading of our already sub-standard and outdated power distribution network becomes necessary. It is proposed in this work that using urban areas as sites for small-scale wind energy generation increases the available locations for wind energy generation and locates the capacity near the demand.

1.2 WIND ENERGY GENERATING DEVICES

The current wind energy market contains primarily two generator types: Horizontal Axis and Vertical Axis turbines. This section presents a description of how each type operates. Also, the prototype AEH being studied is described as it converts wind energy into electric current in a different manner than the other two types of wind turbines.

1.2.1 Horizontal Axis Wind Turbine

The Horizontal Axis Wind Turbine (HAWT) is the most common form of wind turbine. These turbines are almost exclusively found on large wind farms, especially in the US. As the name implies, the turbine consists of either two or three blades which rotate around a horizontally situated shaft. Wind flowing past the blades causes the blades and shaft to rotate. Rotation of the shaft is amplified through a gearbox connected to a generator, which creates the electric current (US Department of Energy, 2009). Large-scale turbines (> 100 kW rated power) are typically connected to the distribution network or ‘grid’ and are thereby integrated into the regional or national electricity supply as is any other generating source. Smaller scale turbines (particularly those owned by individuals) may be connected to the grid, but are more typically used as a supplement to grid-delivered power. Excess power may be stored in batteries or returned to the grid through the use of a transformer arrangement.

HAWTs must be facing into the wind in order to operate. This requires a yaw mechanism to allow the turbine to rotate to face the wind. Frequent direction changes in the wind do not allow for the turbine to rotate quickly enough to face the wind, thus reducing the power output.

Large-scale HAWTs (Figure 1.4a) consist of very tall towers and large blades, which results in high construction and transportation costs. The deployment of HAWTs at appropriate sites (offshore, along ridge lines, etc.) is also fraught with political issues.

Smaller scale, building mounted wind turbines have also been deployed (Figure 1.4b). Aerovironment's (Aerovironment, 2009) Architectural Wind™ AVX 1000 small-scale turbine has been installed at multiple locations, including a Kettle Foods factory in Beloit, Wisconsin and at Boston's Logan International Airport. The airport is the first commercial airport to generate electricity using wind turbines. The AVX 1000 has a 1000W rated power, cut-in speed of 2.2 m/s, and operates at peak efficiency at 10 m/s. These are currently available only to commercial structures, costing \$100,000 for a set of 12 turbines. The SWIFT wind turbine (Swift, 2009) has a 1500W rated power, with a cut-in speed of 2.4 m/s while producing a peak output of 1500W at 14 m/s. This turbine is available for both commercial and residential installation, costing between \$10,000 and \$12,000 for purchase and installation.

While these small-scale turbines have the potential to produce a significant amount of electricity, the biggest drawback of the turbines is the need for high wind speeds to produce near or at their maximum output. At the advertised cut-in speeds, these turbines are only producing a fraction of what they are capable of. With lower wind speeds inside urban districts, it is likely these turbines will rarely reach their optimum output levels, making it harder to recoup the initial investment.

1.2.2 Vertical Axis Wind Turbine

A Vertical Axis Wind Turbine (VAWT) is another type of turbine. These turbines can resemble an egg beater (Figure 1.5a), consisting of a vertical shaft around which at least two vertically oriented blades rotate around (Figure 1.5b and c). These blades are designed similar to airplane wings, one side flat and one curved. However, instead of taking off vertically like airplanes, the lift created from wind flow causes these blades to rotate around the shaft they are connected to. One consequence of this arrangement is while one blade may be rotating with the wind flow, at the same time another one is rotating into the wind direction, which reduces the efficiency of these turbines.

VAWTs do offer some advantages over their HAWT counterparts. The turbines do not need to be pointed into the wind to operate; sufficient wind approaching from any direction will rotate the blades. As a result they do not require a yaw mechanism to direct the turbine into the wind direction. Additionally, VAWTs are often installed at lower elevations, with the gearbox and generator located near the ground surface, making maintenance easier. A disadvantage coming from this low installation is that wind speeds are significantly lower closer to the ground, which will reduce the output of the turbine.

1.2.3 Aeroelastic Energy Harvester

An AEH is a new type of wind energy generator, nothing like the previous two turbines described. This belt operates under the principle of aerodynamic flutter of a strip of thin flexible material, the prototype in this study currently uses Mylar-coated taffeta tape. The tension in the

belt can be adjusted to optimize the efficiency based on wind conditions. At the ends of the belt a copper wire coil and magnet assembly is fastened. This assembly converts the vibration of the belt into an electric current. While this is just a prototype, future assemblies propose the introduction of piezoelectric material, providing for output increases.

Commercial realization of AEH technology has been by Humdinger wind LLC (Humdinger, 2009). There are currently three variations of their AEH, commercially referred to as a ‘windbelt’, reported below and in Table 1.2.

Micro windbelt: intended to power wireless sensors located in an environment where airflow is available such as in HVAC ducts, air-quality sensors, or sensor mounted on a large structure such as a bridge. These belts generate 100-200 watt hours (Wh) over their 20 year life and are conditioned to convert their AC generated signal to 3VDC.

Medium windbelt: intended to provide local power source for wireless repeating stations, exterior lighting fixtures and other similar applications. The medium windbelt is an adjustable length belt (1-3 m) reported to be able to attain output levels of 3-10W.

Large windbelt: Humdinger is reportedly investigating the scalability of their windbelt. Conceptually, large windbelts effectively act as stay cables to a central tower (Table 1.2). The aerodynamic flutter of the ‘stays’ is captured as in the smaller windbelt designs.

AEH design, research, and development is currently ongoing in the Mechanical Engineering department at the University of Pittsburgh. Dr. Lisa Weiland, Dr. Daniel Cole, and Mechanical Engineering graduate student Tim Bagatti are experimenting with various setups in order to increase the efficiency and output of a prototype AEH. The most current version of their AEH is shown in Figure 1.6a. The current version of this AEH is a single belt with 2 copper wire coils and 2 high strength magnets located at each end of the tensioned belt (Figure 1.6b). A

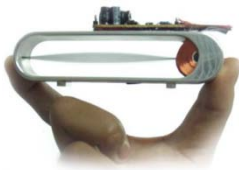
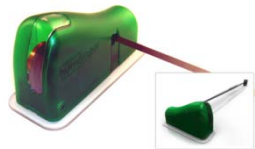
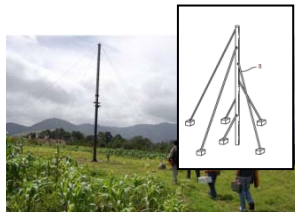
second taffeta belt shown in the image is presently being studied however there is no data available for this. This project is in its early stages and results are very limited at this point. Preliminary results show the AEH generates 50 mW at a wind speed of approximately 2 m/s. Although the output is small, a benefit of this AEH is the very low operating speed. This will potentially allow for a wider range of installation possibilities, including urban areas where HAWTs and VAWTs are not viable due to their need for high wind speeds in order to operate at peak efficiency and output.

While developments at Humdinger are aimed at optimize the power output of their windbelt in order to move into a commercial market, Dr. Weiland, Dr. Cole, and Mr. Bagatti are primarily focused on populating a model to predict outputs of the AEH. The model created will allow for true optimization as opposed to a trial and error approach of product development. Further information on the development of this model can be found in Cole (2009). The paper examines how Aeroelastic Energy Harvesters generate power and the equations that describe the motion of the device.

Table 1.1: Wind Power Classes (U.S. Department of Energy, 2009)

Wind Power Class	Wind Power Density at 50m (W/m ²)
1	0-200
2	200-300
3	300-400
4	400-500
5	500-600
6	600-800
7	800+

Table 1.2: AEH from Humdingerwind.com (Humdinger, 2009)

	micro windbelt	medium windbelt	large windbelt
all images from humdingerwind.com			
cut in wind speed	2.7 m/s		no data available
operational wind speed	2.24 – 8.94 m/s		
rated power		3-10 W	
energy	100-200 Wh		
AC frequency	70 Hz	50-60 Hz	
conditioning	to 3VDC		
life span	20 years		
cost		\$2/W	

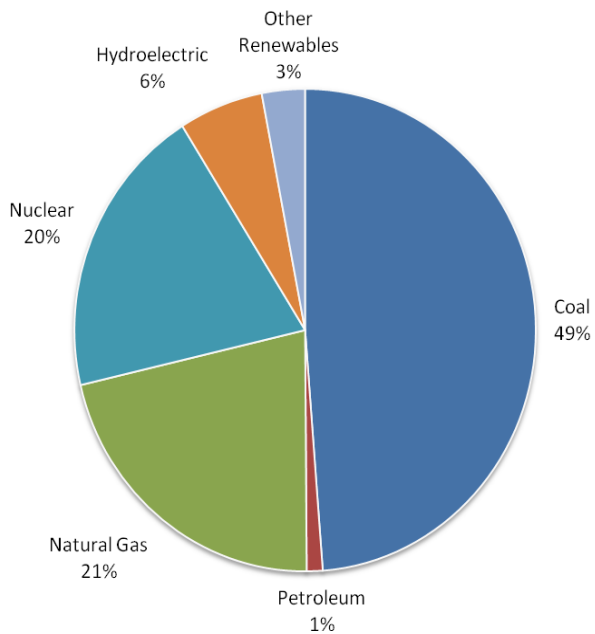


Figure 1.1: US Electricity Net Generation, 2008
(Energy Information Administration, 2009)

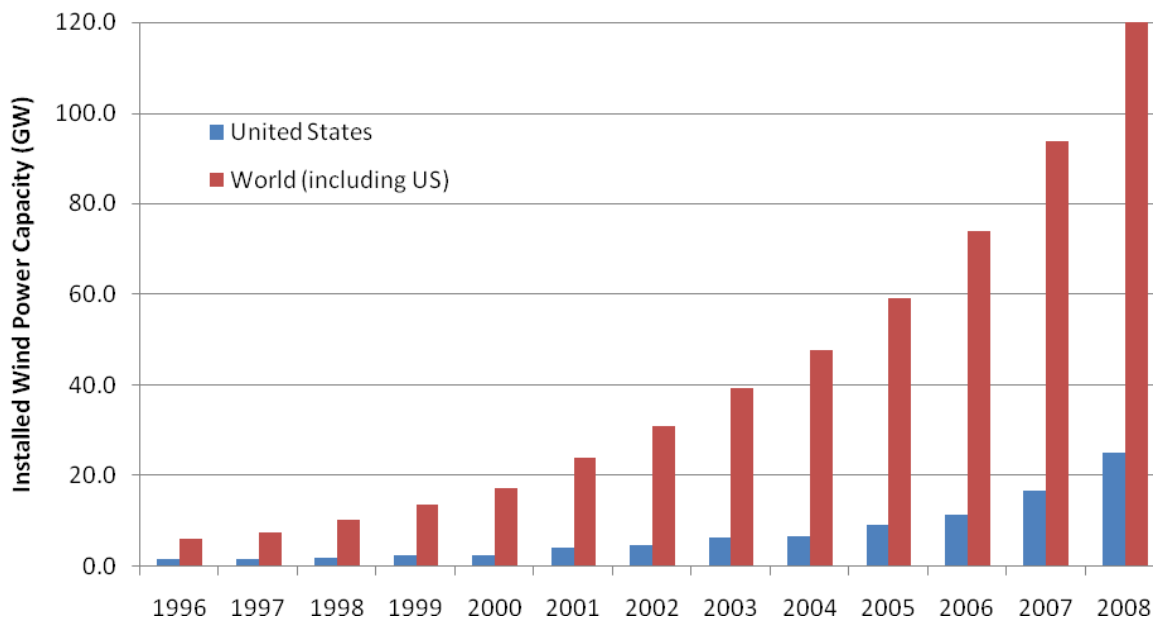


Figure 1.2: Cumulative Installed US and World Wind Energy Capacity (GW)
(GWEC, 2008)

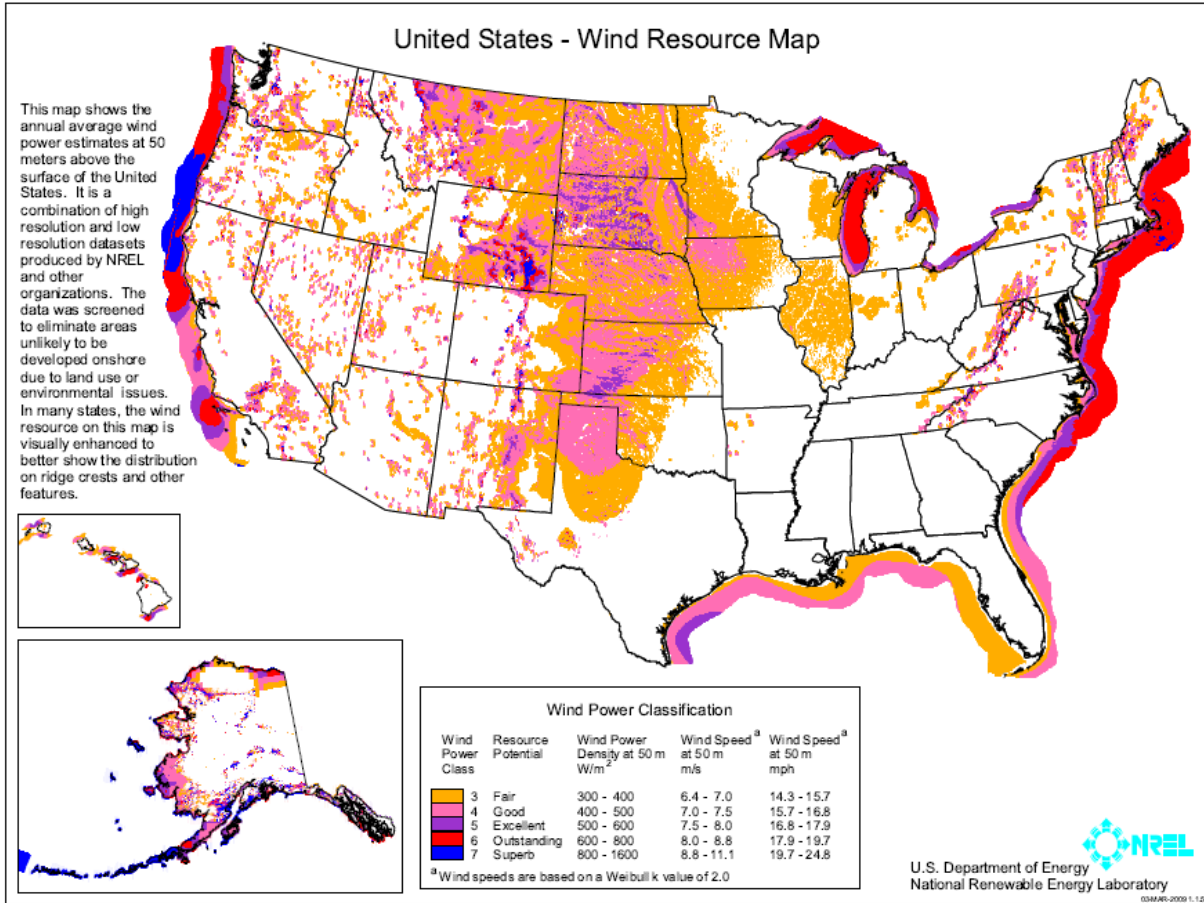


Figure 1.3: US Wind Power Class Map (US Department of Energy, 2009)



(a) World's largest HAWT, the Enercon E-126. Power capacity of 6 MW, can produce 20 million kWh of electricity, enough to power almost 1800 average US homes per year. Rotor blades are 126 m long. (photo: newlaunches.com)



(b) Aerovironment's AVX1000 small-scale wind turbine mounted along a parapet at Kettle Foods manufacturing facility in Beloit, Wisconsin. 18 turbines projected to generate 28,000 kWh/year. (Photo: renewableenergyworld.com).

Figure 1.4: Examples of Horizontal Axis Wind Turbines (HAWT)



(a) 'eggbeater' VAWT
(Quiet Revolution)

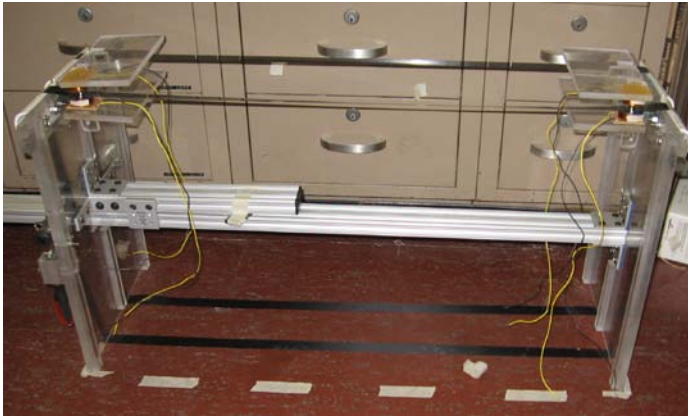


(b) three-blade VAWT
(Photo: cnet.com)

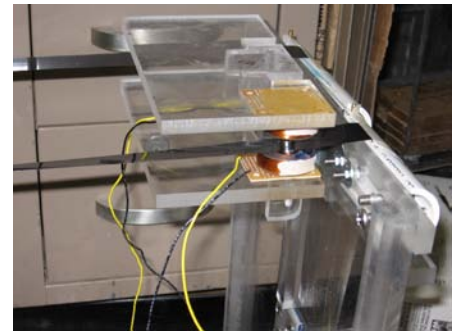


(c) six-blade VAWT
(Alvesta)

Figure 1.5: Examples of Vertical Axis Wind Turbines (VAWT)



(a) Most recent progress on the AEH at the University of Pittsburgh. The current results come from a single belt setup (front). The second belt (back) on the AEH is another option being studied, but no results are available currently.



(b) Close-up of copper wire coil and magnet apparatus. As the belt vibrates, magnets attached both above and below the belt move in and out of the solenoid, creating a current.

Figure 1.6: Current Progress on AEH at University of Pittsburgh

2.0 LITERATURE REVIEW

2.1 LIFE CYCLE ASSESSMENT

Life Cycle Assessment (LCA) is a tool used to assess the environmental impacts of a product, process, or industry. As the name suggests, LCA takes into account the entire life cycle, including raw material extraction, manufacturing, use, decommissioning, and disposal, of whatever is being studied. The guidelines for performing a Life Cycle Assessment are described by the International Organization for Standardization (ISO 14040). There are four primary stages in an LCA: goal and scope definition, inventory analysis (LCI), impact assessment (LCIA), and interpretation.

Defining the goal and scope of an analysis is the first step in performing an LCA. In this step the purpose, audience, system boundaries, and functional unit are all defined. The system boundaries show what processes will be included in the LCA. This is usually modeled through a simple flowchart. Often times, the study will not include every single step that goes into the subject being studied due to time restrictions or lack of data. The functional unit is a quantitative unit that is used to relate the various impacts of the product. An example of a functional unit is kWh for electricity generating technologies. For stand-alone studies, the functional unit is rarely a critical decision. However, when performing a comparative study, the functional unit must be chosen in a way that the options being compared are compared in a fair and reasonable way.

The Life Cycle Inventory (LCI) step is often the most robust and time consuming portion of an LCA. The three steps in completing an LCI are: 1) Construction of a flow chart based on the defined system boundaries, 2) Collecting data for the included activities inside the system, and 3) Calculating the environmental loads in relation to the functional unit defined in the first step of the LCA (Baumann and Tillman, 2004). The initial flowchart created in the goal and scope phase is now expanded on, showing in detail the activities to be studied and the flows between them. Data collection is the most time consuming portion of performing an LCA. Both qualitative and quantitative data reflecting such things as material amounts, energy use, and transportation is researched and documented. Once the data has been collected and recorded, the environmental loads can be calculated.

Life Cycle Impact Assessment (LCIA) is defined as a qualitative and/or quantitative analysis of outcomes such as environmental and human health-related effects or anticipated product/process lifetime and payback period, the time required to recover the initial investment, associated with resource use (Fava et al., 1991). In the LCIA stage, there are three primary steps: classification, characterization, and normalization. Classification is assigning the inventory items to impact categories, such as acidification, global warming potential, and ozone depletion. Characterization is describing the impacts in comparable units (i.e. the functional unit) within each impact category. Normalization consists of taking the data and relating it to a reference value. Typically one option being considered will serve as the basis for normalization and thus be assigned a value of unity allowing for comparison across multiple impact categories.

The final step of an LCA is interpretation. It is the phase where the LCA conductor can present conclusions, make recommendations, and point out areas in the LCA in need of

improvement. This step can either be completed after the other three steps have been finished, or be used in an iterative fashion, following the completion of each step.

2.2 WIND ENERGY GENERATION ENVIRONMENTAL IMPACTS

This section describes the various studies examining the environmental impacts associated with wind energy generation. A common misconception is that wind power produces ‘clean or carbon-free’ energy. LCA studies of wind turbines show that there are impacts associated with wind power. Few LCAs have been performed for wind turbines, large or small, and the majority of the studies are based on European data and sites; the United States has not been the geographic location of these studies as LCA is still very new to the US. There are three topics the majority of the studies address: environmental impacts (mostly CO₂ emissions), lifetime of turbine, and payback period. Payback period is especially important as small-scale wind power (which may have shorter product lifetimes) will never find its way into the market if it is not economically viable.

2.2.1 Large-Scale Wind Turbines

While many of the studies focusing on small-scale turbines deal primarily with carbon dioxide emissions, one study, however, presented the LCA of a large-scale wind turbine considering many more impact categories. The study (Martinez et al., 2009) analyzed the impacts of a 2 megawatt (MW) horizontal axis wind turbine (HAWT) located at a wind farm in northern Spain.

The turbine was assumed to produce 4 gigawatt hours (GWh) annually and the functional unit used in the study was kWh. This functional unit selection allows for a relatively easy comparison between other types of energy generation methods. The four main physical components of HAWTs are the base, tower, nacelle, and rotor. The nacelle houses the transmission and turbine that converts the rotational energy into electrical power. Similar to other LCAs, this study focused on four stages of the wind turbine: manufacturing, transportation, use, and disposal. The study presented results for many environmental impact categories, including organic and inorganic respiration, global warming potential, and fossil fuel use. The results show the manufacturing stage to be the largest contributor to many of the impact categories, especially inorganic respiration and fossil fuel use. Within the manufacturing stage, the concrete foundation of the turbine has the largest environmental impact. For small-scale turbines, this large impact may be mitigated since the foundation volume will scale approximately with the square of the turbine size (that is, a turbine having half the height and blade diameter will require a foundation only one quarter the size). One difficulty in interpreting the results of the study is that they are presented in terms of “Eco-points”, which are never truly defined in the paper, thus the true impact of each phase cannot be compared with that of another study.

In the same study (Martinez et al., 2009), the payback periods for both input energy as well as the other impact categories were analyzed. The wind turbine was assumed to operate for 2000 equivalent full-load hours (EFLH) – approximately 23% capacity – per year. The EFLH accounts for the wind environment and maintenance requirements. Based on a 20 year life span, the energy payback time was found to be just under half a year. Each impact category’s payback period was calculated based on their “Eco-point” values. The results ranged from 22 days for carcinogens to having a payback time greater than the 20 years for the radiation, land use, and

minerals categories. However, since these eco-points are not well defined, it is difficult to draw conclusions based on this data.

Two separate studies (Hondo, 2005; Weisser, 2007) summarized the life cycle greenhouse gas (GHG) emissions of many power generating technologies, including large-scale wind power. The earlier study by Hondo, presented two cases: the base case was an LCA of a 300 kW on-shore turbine and the future case was a more sophisticated 400 kW on-shore turbine. For both cases it was assumed the electricity was exported to the grid. No specific details on the procedure used for this LCA were given, only results, which adds uncertainty to their interpretation. The 300 kW turbine was found to emit 30 g-CO₂/kWh over the course of its 30 year life, with 72% coming in the construction phase, while the 400 kW turbine resulted in 20 g-CO₂/kWh being emitted with 70% coming from construction. The emissions caused by the wind turbines are all considered indirect as they are not caused by the electricity generating process. Coal power GHG emissions, on the other hand, are largely direct as the burning of coal produces the electricity but also produces the majority of the emissions. The study also presented the GHG emissions as a function of lifetime and the capacity factor of both turbines. The analysis held one variable constant while studying the effects of changing the other. This showed that the 400 kW future case wind turbine with an assumed 100 year lifetime would emit the lowest amount of GHG (10 g/kWh). However, this seems to be unrealistic as the odds of a wind turbine operating at a constant capacity factor for 100 years are very low.

The study performed by Weisser (2007) presented a range of GHG emissions compiled from multiple published LCA's of turbines. The turbines studied were all large-scale turbines. According to the author, between 70 – 90% of emissions caused by wind turbines can be attributed to the turbine production and the construction of the foundation. The compilation of

LCA studies of wind turbines resulted in a range of 8 – 30 g CO₂/kWh emitted. Turbine location, capacity factors, and lifetimes all add to the variation seen in these results.

2.2.2 Small-Scale Wind Turbines

In the studies of small-scale wind turbines, the focus appears to center primarily on CO₂ emissions and the other impact categories are not presented. The following studies give a sample of the environmental impacts of small-scale wind turbines.

Allen et al. (2008) performed an LCA of a 600 W horizontal axis turbine installed for residential use. The study focused on determining a range of potential electricity outputs, life cycle emissions, and saved emissions based on the current UK grid electricity mix. Since wind is an intermittent resource, a minimum, maximum, and average output value were determined for both an ‘urban’ and ‘open’ setting. In the study, ‘open’ meant the wind turbine was installed on a 10 m tall mast away from rural households and ‘urban’ meant the turbine was to be installed on a building also at a height of 10 m from the ground. Wind speed data was collected from multiple urban and open locations and annual mean wind speeds determined (2.8 – 7.8 m/s open; 2.3 – 5.2 m/s urban). Turbulence was assumed to reduce the possible power output by 15% in the open field location and by 50% in the urban location. This resulted in an annual energy output range of 250 – 1500 kWh at the open location and 50 – 250 kWh at the urban location. Since 2000, the average UK family consumes approximately 4500 kWh of electricity. Therefore, the mean energy output from the open location turbine provides 20% of the demand while the output from the urban location only provides 4%. The study utilized the LCA software program SimaPro v.7

(Pre Consultants, 2007). The energy and water use from the factory where the turbine was manufactured was omitted from the study as the data was unavailable. While this step may not have a large impact on the results, a substitution could have been made utilizing general manufacturing data. The other phase omitted was the decommissioning and disposal of the turbine. This is standard at this point in time as almost no information is available on the process of disposing of wind turbines since they have only recently been utilized on a large-scale. In almost all impact categories (global warming, heavy metals, carcinogens, etc) the main contributor was the component that was used to attach the turbine to the building. This part was made from aluminum, which is a highly energy intensive material. One set of results showing the true values of each impact category were presented in units of ‘people emission equivalents’, which is defined as “emissions from the process studied/European emissions per capita”. This approach is somewhat confusing and it seems the results would be easier to analyze had they been presented in units such as kg/kWh. Unless another paper presents their results in terms of ‘people emission equivalents’, making comparisons between studies will be very difficult.

In addition to the ‘people emission equivalent’ results, the study also presented results of the turbine production for each impact category in the standard impact category units i.e. kg CO_{2eq} (CO₂ equivalents: see section 3.3) for global warming. Each of the impact categories was compared to the potential savings from avoiding electricity provided by the UK electric grid. The energy produced by the turbine was presumed to offset the amount of energy needed by the UK grid to deliver the same amount of energy to the end user. The results for the ‘urban’ location are shown in Table 2.2. The negative values in the table are the savings that result from avoiding using grid electricity based on the output levels of the turbine.

Rankine et al. (2006) performed an LCA of a 1.5 kW roof-mounted 'SWIFT' wind turbine. The goals of the study were to determine both energy and CO₂ payback periods. The functional unit was appropriately chosen as kWh. The turbine was assumed to produce anywhere from 1000 to 4000 kWh annually, which corresponds to a capacity factor range of 8 – 30%, and mean wind speeds between 4 and 7.2 m/s. Using a weighted average of CO₂ emissions of the various fuel sources in the UK electricity mix, the carbon intensity of UK electricity was found to be 504 g CO₂/kWh. This would result in annual savings of 500 – 2000 kg CO₂ per SWIFT turbine. The life cycle portion of the study presented one set of results in terms of energy consumption (MJ/kg) and CO₂ emissions (kg CO₂/kg) related to the manufacturing of the turbine. Data for the LCA were primarily taken from the relevant industry's own life cycle studies. Due to the numerous parts and processes of producing the turbine, certain stages were either omitted or data was substituted with similar industry data. In many of the cases assumptions were made, it was expected these would not have a large impact on the results.

One key finding showed that aluminum, which accounts for 70% of the turbine's weight, consumed 77% of the 22,829 MJ of energy required throughout the complete life cycle of the turbine. In terms of provided results based on the functional unit, the study presented these as a range based on the expected electrical output of the turbine (1000 – 4000 kWh). In addition to this, the results were presented with and without a 30% recycling credit. The life cycle energy intensities of the turbine varied from 195 kJ/kWh (4000 kWh annual production with recycling) to 1140 kJ/kWh (1000 kWh annual production with no recycling). Similarly the life cycle carbon intensities of the turbine ranged from 20.7 g CO₂/kWh to 121.4 g CO₂/kWh. To determine the carbon payback time, the life cycle CO₂ production was divided by the total CO₂ saved by not consuming the grid electricity. The calculated energy payback period ranged from 13 – 74

months depending on turbine output and recycling, while the CO₂ payback time ranged from 10 – 58 months. In this study, an extensive review of LCA's of wind turbines performed by Lenzen and Munksgaard (2002) was referenced providing ranges of energy and carbon intensities: 50 – 3650 kJ/kWh and 8 – 124 g CO₂/kWh, respectively. The results in Rankine's study place the SWIFT in the lower portion of these ranges.

The last stage of the study by Rankine et al. (2006) performed a sensitivity analysis, replacing the aluminum parts with a) recycled aluminum and b) steel. Recycled aluminum was chosen because of the significant reduction in its embodied energy compared to virgin aluminum (31.7 MJ/kg vs 213.5 MJ/kg). Steel production requires a similar amount of energy as recycled aluminum which is why it was chosen as an alternative as well. Using the recycled aluminum resulted in a 65% reduction in energy payback time and a 30% reduction in the CO₂ payback time. The use of steel as a replacement resulted in reduced payback times (30% for energy and 15% for CO₂), proving both to be potential alternatives. This LCA, while being quite thorough, showed the need for research of the disposal and decommissioning of wind turbines.

Although a full LCA was not performed in a study by Peacock et al. (2008), an analysis of potential mitigated CO₂ emissions was conducted on four small wind turbines (0.4 kW, 0.6 kW, 1.5 kW, and 2.5 kW). Each turbine was assumed to have a 20 year life span and operate at maximum efficiency at wind speeds of approximately 15 m/s. Mean wind speeds were calculated at two sites in the UK. Site A had average wind speeds of 4.9 m/s and was called the "high" site. Site B had average wind speeds of 2.0 m/s and was called the "low" site. These wind speeds resulted in the turbines operating below their maximum power output. The turbines at the low site produced no electric output 51 – 70% of the time, depending on the turbine. At the high site, the turbines fared better, but still produced no output 25 – 37% of the time. This highlighted a

key issue in small-scale wind turbine technology; wind turbines often have cut-in speeds (minimum speed the turbine needs to produce electricity) that are not consistently reached in an urban/residential setting. Also, these turbines often produce at maximum efficiency when operating under strong wind conditions (>10 m/s), which is not often found inside an urban area. In terms of energy production, none of the four turbines at either site produced enough electricity to fully supply the typical household, with the turbines producing anywhere from 80 kWh to 4900 kWh annually.

Each kWh produced by a turbine was assumed to save 430 g CO₂ by avoiding electricity generated by the UK electric grid. The annual CO₂ savings at the low site were very minimal: 32 kg for the 0.4 kW turbine and 160 kg for the 2.5 kW turbine. At the high site, the CO₂ savings increased, ranging from 244 – 2098 kg depending on turbine power rating. The study shows the significance of small wind speed increases on turbine output and therefore, on CO₂ savings.

Currently, there are no known LCA studies of AEH generators.

2.3 WIND ENVIRONMENT

In order to determine viability of a small-scale wind energy generator, knowledge of how wind flows inside the lower portion of the atmosphere is necessary. There are two types of flow that will be focused on in this section: open field flow (i.e. rural areas) and flow in an urban environment.

2.3.1 Open Field Flow

In open terrain with relatively few obstructions, wind profiles are much simpler than in urban districts. There are two conventional ways to model the mean wind profile in rural areas with homogeneous terrain; using a power law (Equation 1) or a logarithmic law (Equation 2).

$$\text{Power Law: } u(z_1) = u(z_2) \left(\frac{z_1}{z_2} \right)^\alpha \quad (2.1)$$

$$\text{Logarithmic Law: } u(z) = \frac{u_*}{k} \ln \left(\frac{z - d_o}{z_o} \right) \quad \text{only valid for } z > d_o \quad (2.2)$$

Simiu and Scanlan (1986) provided a variation of the power law, calling it the “Power Law Model” (Equation 3) which provided a way to relate velocities at two locations, taking into account height and roughness length of the two locations.

$$\text{Power Law Model: } u(z_1, z_{o1}) = \left(\frac{z_1}{\delta(z_{o1})} \right)^{\alpha(z_{o1})} \left(\frac{\delta(z_{o2})}{z_2} \right)^{\alpha(z_{o2})} u(z_2, z_{o2}) \quad (2.3)$$

In Equations 1 – 3:

$u(z_i)$ = velocity at elevation z_i

u_* = friction or shear velocity, which is a function of the surface shear and air density (Simiu and Scanlan, 1986)

d_o = displacement height, defined as the elevation where the mean wind speed converges to zero due to the surrounding flow obstacles

z_o = roughness length, defined as a corrective measure that accounts for the roughness of a surface; generally between 2-3 meters for cities (Oke, 1988)

α = coefficient dependent on roughness of terrain; recommended values for urban terrain are $\alpha = 0.14$ (ASCE 7-05) and $\alpha = 0.16$ (Davenport 1965); $\alpha = 0.28$ for suburban terrain (Davenport, 1965).

k = von Karman coefficient typically taken as $k = 0.4$ (Kastner-Klein and Rotach, 2004).

$\delta(z_{oi})$ = depth of ‘surface layer’ based on roughness length z_{oi} ; recommended values for urban terrain are 366 m (ASCE 7-05) and 520 m (Davenport, 1965). Recommended values for open terrain are 275 m (ASCE 7-05, Davenport 1965).

$u(z_i, z_{oi})$ = wind speed at height z_i over terrain with roughness length z_{oi} .

2.3.2 Flow in the Built Environment

Once wind flow reaches an urban boundary, the profile becomes much more complex as there are many more variables affecting the wind profile. The interaction of the open field wind profile with the increased surface roughness associated with an urban environment causes multiple layers to form within the Urban Boundary Layer (Ricciardelli and Polimeno, 2006), as shown in Figure 2.1. For studying potential placement of a device, the most important layers are the Roughness Sublayer (RS) and the Canopy Layer (CL). According to Mertens (2003), the wind profile in an urban area above the RS will be approximately equal to the wind speed upwind of the roughness change. The growth of the RS is shown in Equation 4. Inside this layer, the wind speed profile follows a more complex logarithmic law (Equation 5).

$$\text{RS Growth: } h(x) = 0.28 z_{o,\max} \left(\frac{x}{z_{o,\max}} \right)^{0.8} \quad (2.4)$$

$$\text{Urban Wind Profile: } u(z_1) = \frac{\ln\left(\frac{h_1(x)}{z_{o,ref}}\right) \ln\left(\frac{z-d_o}{z_o}\right)}{\ln\left(\frac{h_{ref}}{z_{o,ref}}\right) \ln\left(\frac{h_1(x)-d_o}{z_o}\right)} u(z_2) \quad (2.5)$$

Where x = horizontal distance from the change in roughness

$z_{o,\max}$ = larger of the upstream and downstream roughness (in Mertens, downstream is always larger); values range from 3 m (Davenport, 1965) to 20 m (Grimmond and Oke, 1999)

$h_i(x)$ = Roughness Sublayer height at length x

$h_{ref} = 10$ m

$z_{o,ref} = 0.03$ m

Equation 4 is only valid up to a height of approximately 200 m (Mertens, 2003).

The RS extends up from the ground to a height of 2 to 5 times the average building height. The wind flow characteristics inside the RS are dependent on building arrangement, with two relevant parameters being 1) how uniform the heights of the buildings are and 2) the urban aspect ratio, defined as the ratio of the average building height to the average street width (H/W).

Based on this ratio, wind behavior can exhibit three separate characteristics:

- 1) $H/W < 0.3$: isolated buildings dominate the wind flow
- 2) $0.3 < H/W < 0.65$: aerodynamic interference between buildings takes place
- 3) $H/W > 0.65$: skimming flow develops

These three flow characteristics are shown in Figure 2.2. Skimming flow occurs in dense urban locations, and a new tier, the Canopy Layer (CL), is formed inside the RS. The CL formation is important since the displacement height, d_o , in Equation 2 is located inside this tier at a height of approximately 65-75% of the mean building height.

As the wind profile moves from a rural/suburban setting into an urban setting, the changes in the mean wind speed are predominantly affected by the changes in average building height and average building density (Coceal and Belcher, 2004). Urban canopies can be effectively described as inhomogeneous canopies, while rural settings are much more homogeneous. As urban areas contain hundreds of buildings, it is not practical to model the flow around each individual building in order to describe a general wind profile; it would require an enormous amount of data, time, and processing power. Currently, modeling the flow inside an urban canopy uses only a single average roughness length, defined as a corrective measure that accounts for the roughness of a surface; generally between 2-3 meters for cities (Oke, 1988). This is an inaccurate procedure for two reasons. First, defining a roughness length is only possible when the wind profile near the surface is a logarithmic representation. Second, because the flow inside the canopy is constantly changing as a result of the built environment, defining a single roughness length is difficult.

Ricciardelli and Polimeno (2006) analyzed wind flow past a 4 x 5 grid of blocks (Figure 2.3a) in a wind tunnel. Each block was 20 x 16 cm in plan and 15 cm tall (i.e. $H = 15$ cm), with 12 cm spacing between each (i.e. $W = 12$ cm). Measurements were taken at 12 elevation levels at 9 locations. All 9 points were located near the center of the grid: 6 in a longitudinal canyon, 2 in a transverse canyon, and 1 directly above a cube (Figure 2.3b). The building aspect ratio of the experiment was $H/W = 1.25$, which resulted in skimming flow. The incident flow was

characterized by a power law profile with $\alpha = 0.28$, which is indicative of suburban terrain (Davenport, 1965), and an undisturbed mean wind speed of 10 m/s. The mean wind speed at a height of 15 cm was measured to be 7.5 m/s without the model in place.

Two variables, mean wind speed and turbulence intensity, were recorded and analyzed at 8 of the measurement locations. The location directly above one block was never reported on. The mean wind speed profiles of the longitudinal and transverse canyon are significantly different (Figure 2.3c and d) Defining z as the variable corresponding to height, the transverse canyon mean wind speed profile is linear from just above $z = H$ to $z = 2H$, but experiences a significant decrease in wind speed at $z = H$ (roof level). At roof level, the mean velocity is roughly 3 m/s, while just above this ($z = 1.2H$) the velocity is 7 m/s. Since wind power is dependent on the cube of wind speed, this significant change will drastically alter the power output of a generator located in this layer immediately above the roofline. In the longitudinal canyon, the wind speed profile is linear for $z < 1.7H$, with a velocity of approximately 5.5 m/s at the roof level and 6.5 m/s at $z = 1.2H$. In the longitudinal canyon, the turbulence intensity and its horizontal scatter increases as the ground is approached (Figure 2.3e). The turbulence intensity in the transverse canyon is both larger and exhibits less scatter than the turbulence in the longitudinal canyon (Figure 2.3f).

Skote et al. (2005) used numerical simulation to study wind flow inside an urban area. The two cases studied consisted of a single street and two streets that intersect, forming a 90° angle with each other. The free flow velocity was set to 10 m/s. Each case was performed with the velocity entering the street channel directly as well as at a 30° angle (Figure 2.4a). For both the single-street and double-street direct entrance cases, the wind velocity increased near the entrance and slowed down as it traveled through the channel (Figure 2.4b). However, when the

velocity hit the channel at an angle, the increase was minimized and vortices developed along portions of the channel (Figure 2.4c). One of the more interesting conclusions from Skote's study is the development of vortices all throughout the perpendicular street channel (Figure 2.4d). The vortices develop at low speeds, but should have an increased amount of turbulence in the areas they occupy.

2.3.2.1 Urban Canopy Model

A method developed as an attempt to address the complexity of the urban wind environment is known as the "urban canopy model" (Coceal and Belcher, 2004). This model includes relevant and suitable parameters for large-scale roughness elements in order to determine average mean wind speeds inside a specified area or along a distance within and above urban canopy layers. Essentially, the model treats the urban area as one large element where the many roughness lengths make up a porous medium for air flow.

While a description of all the variables that make up this method are not inherently important for this study, a few of the parameters this model takes into account include the mean drag coefficient for the number of obstacles studied, the roughness density (total frontal building area per unit of ground area), and displacement height, which is the height at which the mean wind speed converges to zero. This value is ranges from $2/3$ to $3/4$ the average building height of the area (Ricciardelli and Polimeno, 2006). A more critical explanation of the parameters used in creating this model can be found in Coceal and Belcher (2005). Many of the variables are related to the building heights and building densities, which appear to have a significant impact on wind flow inside these canopies. An urban district will have a very complex building layout; this model attempts to take this into account when dealing with the mean drag coefficient value. This

value will obviously change from city to city, but there are current studies that have focused on wind flow past set ups of staggered blocks (Coceal et al. 2006 and 2007). These studies have led to finding ranges of certain variables used in the canopy model.

The results of this model based on various inputs and examples give insight as to how the wind profile alters once it reaches the urban canopy. The mean wind velocity profile sharply decreases as it transfers from an open area into an urban district. This decrease is approximately 40-50%. As Figure 2.5 shows, the velocity profile will remain approximately constant throughout the urban area, increasing only when the wind flow has exited the urban district.

2.4 ISSUES AFFECTING SMALL-SCALE WIND TURBINE SITING

Currently there are only a few classifications of small-scale wind turbines being used in the built environment. They are Horizontal Axis Wind Turbines (HAWT) and Vertical Axis Wind Turbines (VAWT). When located on a building, they can be placed into the broader category of Building Augmented Wind Turbines (BAWT). A BAWT can be located in three places: on top of or alongside a building, in between diffuser shaped buildings, or inside a duct of a building (Mertens, 2002).

Installing small-scale wind turbines in the built environment presents a new set of siting problems that large-scale turbines (located in an open field) do not have to address. As stated previously, the average wind speed inside an urban area is significantly (40-60%) lower than the average of open field locations. This makes the site selection for a turbine or group of turbines even more critical.

2.4.1 Bluff bodies and concentrator effects

In order to optimize the energy production of a small-scale wind generator, these power generating devices must make use of a building's ability to act as a concentrator of the wind. Locally, buildings can increase the wind speed by roughly 1.5 to 2 times (Lu and Ip, 2009) as the wind 'deflects' over and around the building. Since the wind power density is a function of the cube of mean wind speed, this can result in an increase of 3 to 8 times the wind power density, typically measured in Watts per square meter (W/m^2). In order to take advantage of this increased wind speed around buildings, the turbine location must not exceed 20% of the relevant dimension (either height or length/width depending on the turbines location) (Mertens, 2002).

One of the more recent comprehensive experiments dealing with concentrator effects is a study using Computational Fluid Dynamics to model wind flow around three scenarios of building setups (Lu and Ip, 2009). The experiment collected wind speed data as well as the turbulence formation around the buildings. Three scenarios were analyzed with the goal being utilization of wind power generation in tall buildings. Scenario A placed two buildings at varying distances from each other (10, 15, and 20 meters apart), scenario B altered the heights of buildings (two identical 70 meter tall buildings and two identical 140 meter tall buildings), and scenario C involved three buildings in a stepped pattern with varying roof slopes: all flat roofs or one roof sloped away from the wind and one sloped into the wind. Taking wind speed data from the Hong Kong Observatory, inlet velocities (range: 6 – 8.5 m/s) for 6 ranges of elevation were used (0-10 m, 10-30 m, etc.) to study the concentrator effects of the building arrangements considered. In both scenario A and B, the wind velocity increased from roughly 6 – 8 m/s up to a maximum of approximately 15 m/s. which occurred at the windward faces primarily in the

channel between the two buildings and then decrease as the wind flows towards the leeward faces. Theoretically, the closer the building spacing, the greater the concentrator effect of the wind flow. In the built environment, however, the spacing between buildings is established by other considerations such as street width. For scenario C, three buildings are arranged in increasing height parallel to the incoming wind flow. Tests are carried out with all flat roofs first, and then tests with the middle roof angled downward away from the wind flow and the last building has a roof inclined upward with the wind. In both cases, the maximum velocity approximately doubles to 14 m/s from the initial velocity. The tallest building is the location with the largest area of this maximum velocity. In the sloped roof trial, the maximum velocity is roughly the same, but is located at the leading edge of the middle building.

At the leading roof edge of a building, the wind velocity vectors in the vicinity of the roof are no longer parallel with the roof, but form an angle with it known as the skew angle (Mertens, 2003). This causes a separation of the flow with the boundary (i.e. the building) and creates a turbulent layer (discussed in the next section). Traditional blade-driven turbine generators lose efficiency in the presence of turbulence.

2.4.2 Turbulence and Flow Separation

Wind in a turbulent state exhibits variable directions of motion instead of moving in a uniform direction with streamlines parallel to each other. Wind flow around bluff bodies tends to increase the turbulence layer that forms near the boundaries of the buildings. For the study reported by Lu and Ip (2009), the magnitude of the turbulent layer forming around the tops and

sides of buildings was recorded. In Scenario A (two identical buildings, altering distance between them), a 10 m turbulence layer formed over the roof and a 6 m layer around the sides of the buildings. Scenario B (two identical buildings of 70 m height and again with 140 m tall buildings) showed similar results. The thickness of turbulence layers forming over the roof and on the sides of the building ranged from 3 m – 15 m between the two cases.

Turbulence layers that form over the roofs of buildings are not uniform along the windward face of the building. The thickness and intensity of the turbulent layer is greatest at the center of the windward edge of the roof and falls toward the roof edges parallel to the wind flow (Kim et al., 2003). Using particle image velocimetry (PIV), the flow around a 3-D model-scale prism inside a wind tunnel was studied. Three planes parallel to the approaching wind flow were studied (Figure 2.6a). In reference to the center line of the prism, the planes were located at $0.0H$, $0.5H$, and $1.0H$. A separation point at the leading and leeward edge of the roof was found in all three planes. This caused recirculation regions to form on the leading edge roof as well as in the vicinity behind the building along the entire height. The size of these regions decreased toward the $1.0H$ plane, as the reattachment point decreased from $1.01H$ along the center line to $0.6H$ along the $1.0H$ plane (Figure 2.6b). These re-circulating regions are where the highest levels of turbulence are found, with the highest being located on the center line plane. The turbulence measurements are of the amount of turbulent kinetic energy (TKE) found inside the recirculation regions. TKE is the measure of mean kinetic energy per unit mass found inside a turbulent flow region.

2.4.3 Wind-induced Pressure

When wind encounters a bluff body, such as a building, it inevitably results in pressure (positive pressure or negative suction) on the façade (cladding pressure) as well as the roof. Dynamic pressure, q , is simply:

$$q = \frac{\rho V^2}{2} \quad (2.6)$$

where ρ = air density and V is the wind velocity

In structural design, to establish design pressures and therefore loads, the open field wind velocity is used and local effects of the wind interacting with the bluff body are described by pressure coefficients. Thus, the design pressure, p , is:

$$p = qC \quad (2.7)$$

Most research dealing with wind induced pressures on buildings has come from wind tunnel studies. However, there has been an increase in field testing related to wind pressures and wind loadings. The field studies typically consist of open field sites and not urban locations. One recent study constructed a 6 m cube in an open field and installed pressure taps in one corner section of the roof for observation (Richards and Hoxey, 2008). This study found the largest average pressure on the roof is located in the vicinity of the leading edge when the wind flow is flowing toward the building at a 45° angle, and the pressure coefficient is negative indicating a suction pressure (uplift). This observation is confirmation of the so called ‘delta wing’ effect and is the cause of numerous low-rise roof failures. This study also presented some of the recorded dynamic pressure values as well as the corresponding instantaneous pressure coefficients, which

were as high as $C = -15$ (suction). These intense pressures often only lasted seconds and did not sustain for long periods of time indicating significant turbulence.

One section of many buildings that has been difficult to measure wind loads/pressures at is the parapet. One study utilized a wind tunnel to study the effects of parapet height on wind pressures (Stathopoulos et al., 2002). The study consisted of two building shapes: a cube ($L/H = 1$) and a shorter building ($L/H = 2$). These were subjected to multiple approach angles of the incoming wind as well as multiple parapet heights. It was found that short parapets ($<0.5\text{m}$) cause a significant increase in the suction pressure on the roof. In addition, altering the wind flow from perpendicular to the building to an incident angle of 45° increased this pressure on the same parapet by an additional 30% for the low-rise building ($L/H = 2$). On the other hand, higher parapets ($>1\text{m}$) resulted in a decrease in these suction pressures. This result confirms the known benefit that parapets have on mitigating uplift forces on roofs provided the parapet is sufficiently tall.

Standard wind design guidelines such as ASCE 7 (2005) provide significant guidance in terms of expected pressure coefficients for a variety of building shapes. Generally it should be understood that regions of a structure having greater pressure coefficients also experience the greatest turbulence and typically delineate the regions where flow separation occurs. An example of a wind pressure coefficient 'map' from ASCE 7 is shown in Figure 2.7 (the example shown is for a hip or gable roof structure).

2.4.4 Wind Power Density

The Wind Power Density (WPD), P , is the measure of the power in the wind per unit area of flow (Yingni, 2006).

$$P = \frac{\rho V^3}{2} \quad (2.8)$$

where ρ = air density and V is the wind velocity

This value is usually reported in units of Watts per square meter (W/m^2). This equation and the different classes of wind power are often utilized in the planning of large-scale projects, usually consisting of horizontal axis wind turbines. The square meter term in the WPD value is the area ‘swept’ by the turbine’s blades as they rotate. WPD is a function of the cube of wind speed, which can significantly alter the potential output with the slightest changes in wind speed.

2.4.5 Current Turbine Performance in Urban Areas

Neither HAWTs nor VAWTs perform well in turbulent layers and should be sited above them: that is, above the ‘canopy’. The reason for their poor performance in turbulence is constant buffeting of the wind onto the turbine blades. This affects the angular momentum of the blades. Additionally, wind from multiple directions can cause physical damage, including fatigue damage, to the blades (Mertens, 2003). Studies of wind turbine performance inside urban districts are very limited, primarily focusing on residential uses and some mid-rise building applications (Dayan, 2006). One study (Mertens, 2003) used CFD information to predict the energy yield of various building and turbine choices. Two examples involved a 2.5kW HAWT

placed on the center of the roof of a 30(l) x 10(w) x 20(h) m urban building. Altering the roughness (function of average building height) produced a doubling of energy yield (1814 kWh/yr to 3757 kWh/yr). The final example kept all variables the same as the more efficient arrangement, only replaced the HAWT with a VAWT. The predicted energy yield of this turbine was 4361 kWh/yr. This increase in energy output was attributed to the improved performance of a VAWT in skewed flow.

2.5 GENERAL CONCLUSIONS FROM LITERATURE REVIEW

From a Life Cycle Analysis perspective, the following conclusions can be made about small-scale wind energy environmental impacts:

1. Of the limited studies performed on small-scale turbines, most only present results in terms of energy and CO₂ payback periods, omitting many impact categories.
2. Turbines that contain high amounts of aluminum in their components show aluminum being a significant contributor to the environmental impacts of the turbines.
3. In regards to CO₂ emissions, both small and large-scale turbines have been found to emit anywhere from 8 – 125 g CO_{2eq} per kWh over the course of a lifetime (15 – 20 years).

With respect to small-scale or local wind-energy generation in an urban environment, the following conclusions are drawn from the foregoing discussion:

1. Compared to open field locations (where most wind data is collected), mean wind speeds inside urban environments are lower, which also reduces the Wind Power Density value.
2. As wind 'deflects' around bluff bodies, concentrator effects can increase the urban wind velocity significantly.
3. These bluff bodies also cause turbulent layers to form in their immediate vicinity. The increase in TKE is a result of rapid changes in both wind speed and direction inside the turbulent layer. The WPD is thus increased due to these higher velocities.
4. HAWTs perform poorly inside turbulent areas as they cannot rotate (yaw) quickly enough to face the rapidly changing wind direction.
5. VAWTs perform better than HAWTs in turbulent layers since they do not need to face the wind to operate, but still are subject to wind buffeting, which weakens or destroys the turbine.

Table 2.1: Small-Scale HAWTs




	D400 (Peacock, 2008) 	(Allen et al., 2008) Image not available	SWIFT (Rankine, 2008) 	Proven Wind Turbine (Peacock, 2008) 
Type of Turbine	HAWT	HAWT	HAWT	HAWT
Rated Power (W)	400	600	1500	2500
Rated Wind Speed (m/s)	16	12	N/A	12
Cut in Speed (m/s)	2	N/A	2.4	2.5
Design Life (yrs)	10-15	15	20	25

Table 2.2: Wind Turbine Impacts and Savings over 15 year lifetime (Allen et al., 2008)

Impact Category	Unit	Turbine Production	Minimum Savings	Mean	Maximum
Greenhouse	kg CO _{2eq}	288	-536	-1420	-2670
Acidification	kg SO ₂	2.01	-2.05	-5.43	-10.2
Eutrophication	kg PO ₄	0.16	-0.13	-0.34	-0.64
Heavy metals	kg Pb	0.02	0.00	-0.01	-0.02
Summer smog	kg SPM	1.84	-1.54	-4.07	-7.68
Winter smog	kg C ₂ H ₄	0.07	-0.04	-0.10	-0.18
Energy resources	MJ	5320	-10200	-27000	-51000
Solid Waste	kg	221	0.00	0.00	0.00

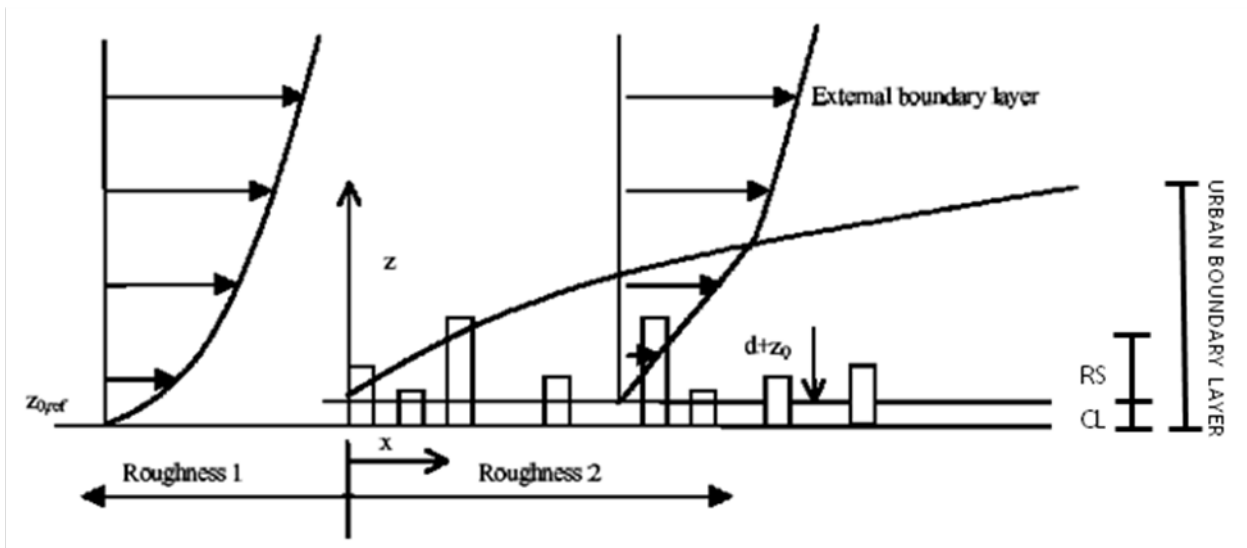


Figure 2.1: Schematic of Wind Profiles (Mertens, 2003)

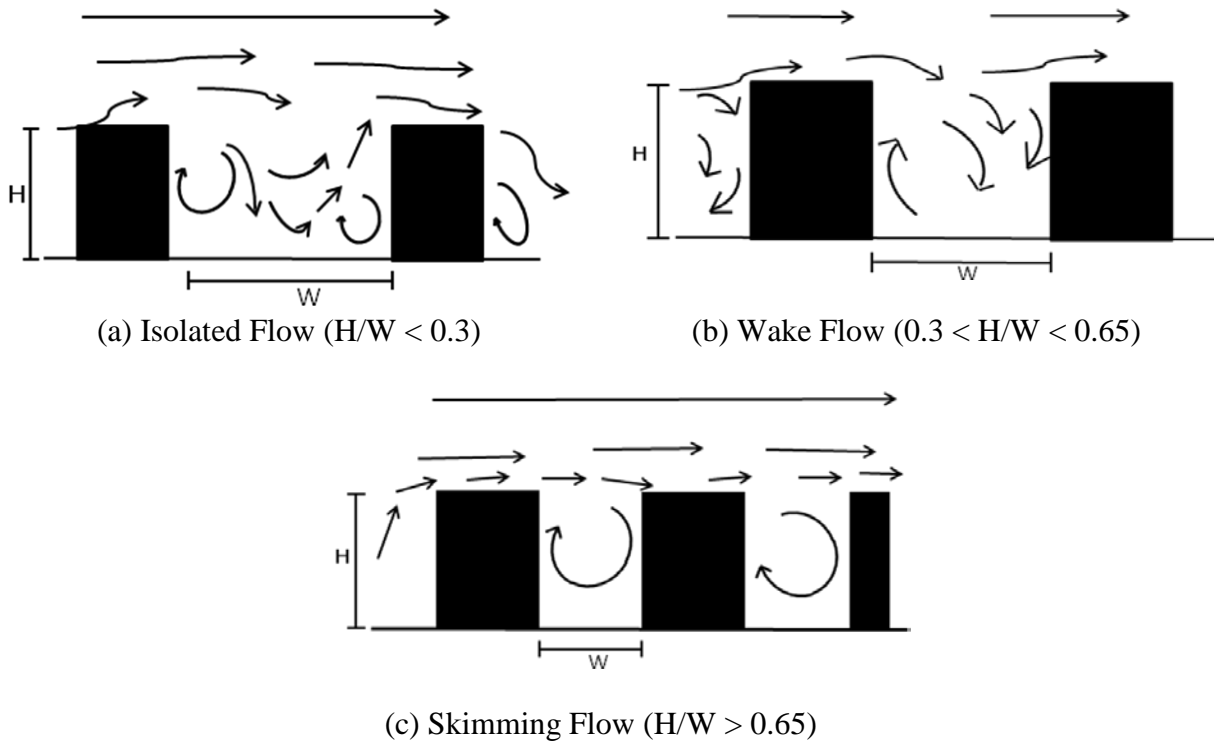
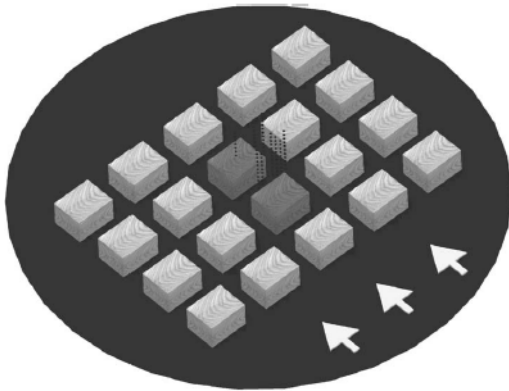
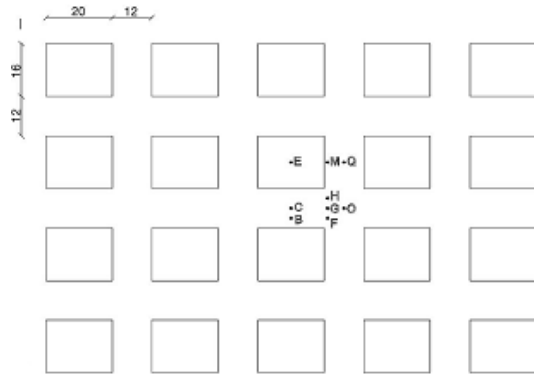


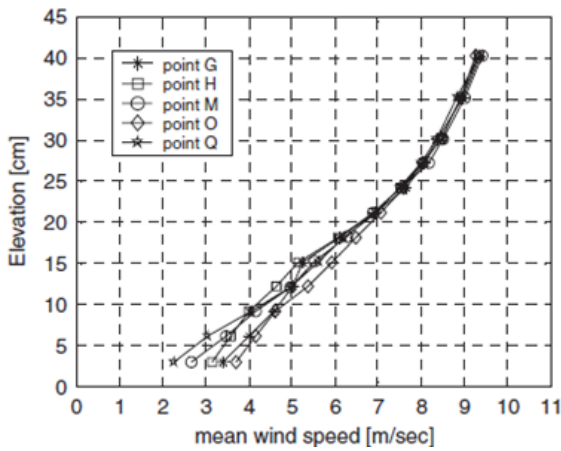
Figure 2.2: Flow characteristics inside RS (adapted from Grimmond and Oke, 1999)



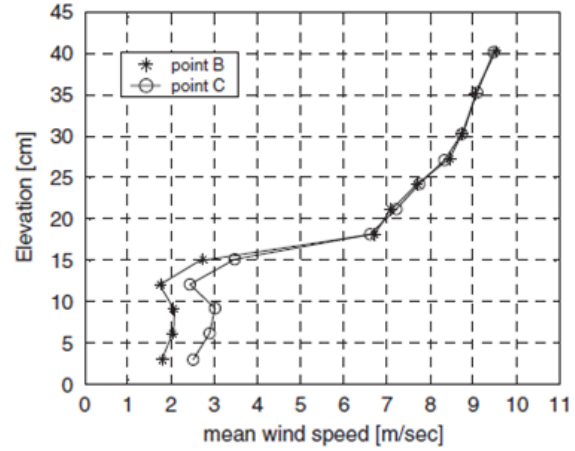
(a) schematic view of test



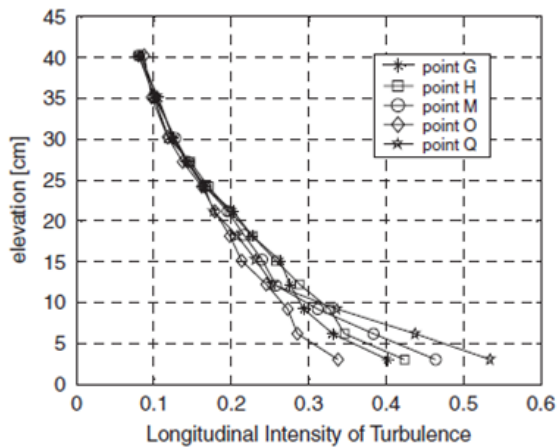
(b) plan view of test and instrument locations



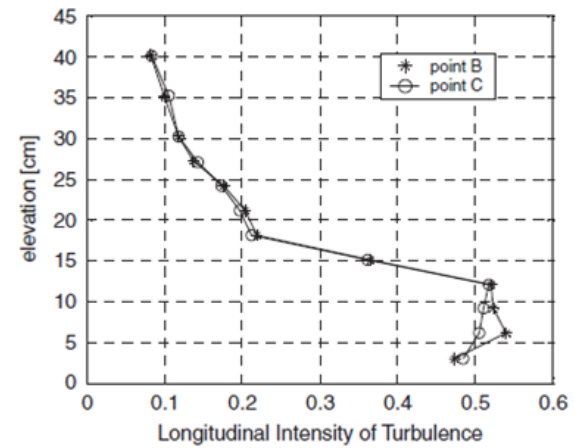
(c) wind profile in longitudinal canyon



(d) wind profile in transverse canyon



(e) turbulence intensity in longitudinal canyon



(f) turbulence intensity in transverse canyon

Figure 2.3: Setup and selected results from Ricciardelli and Polimeno (2006)

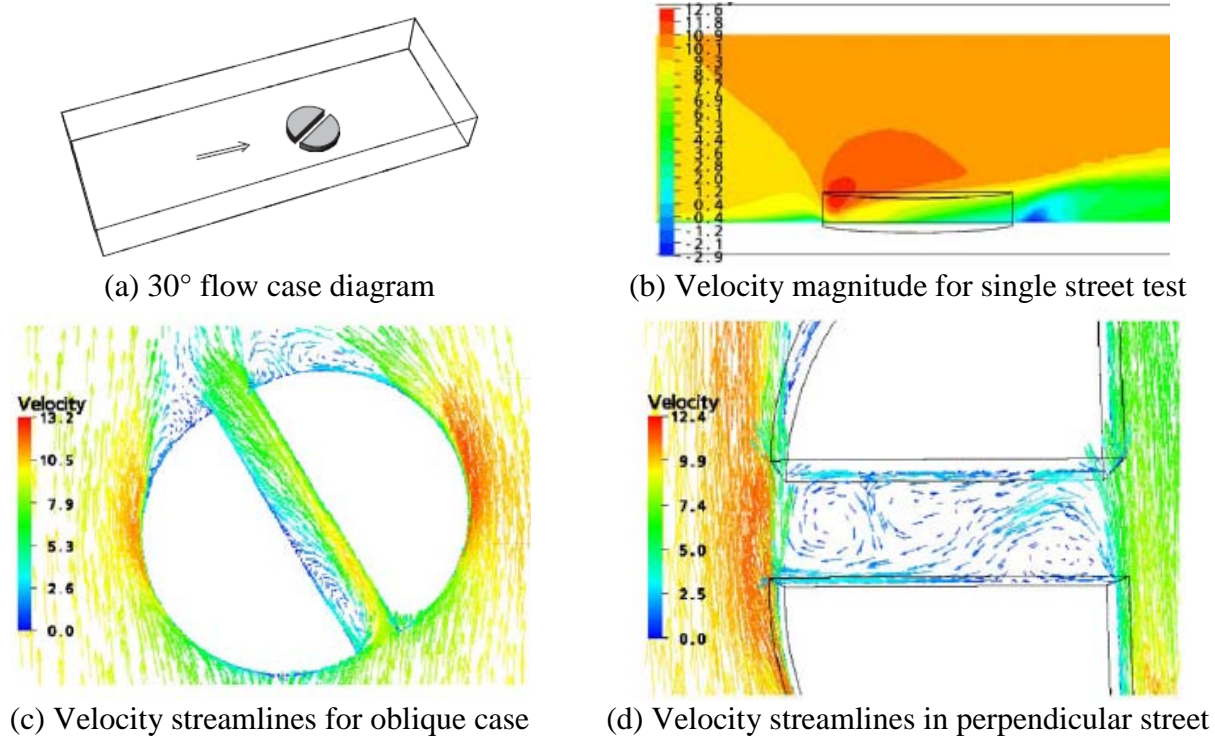


Figure 2.4: Results from Skote et al. (2005)

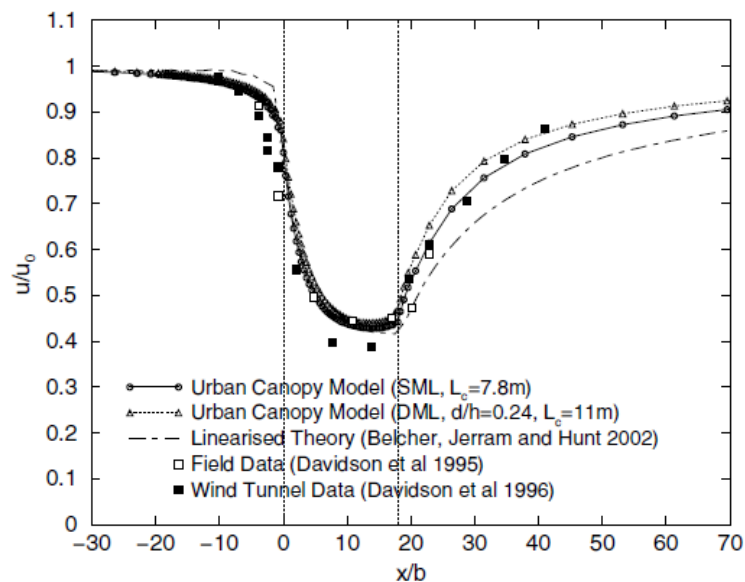
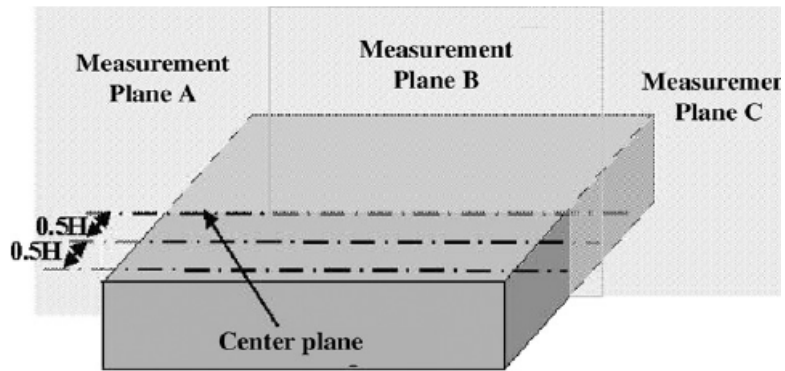
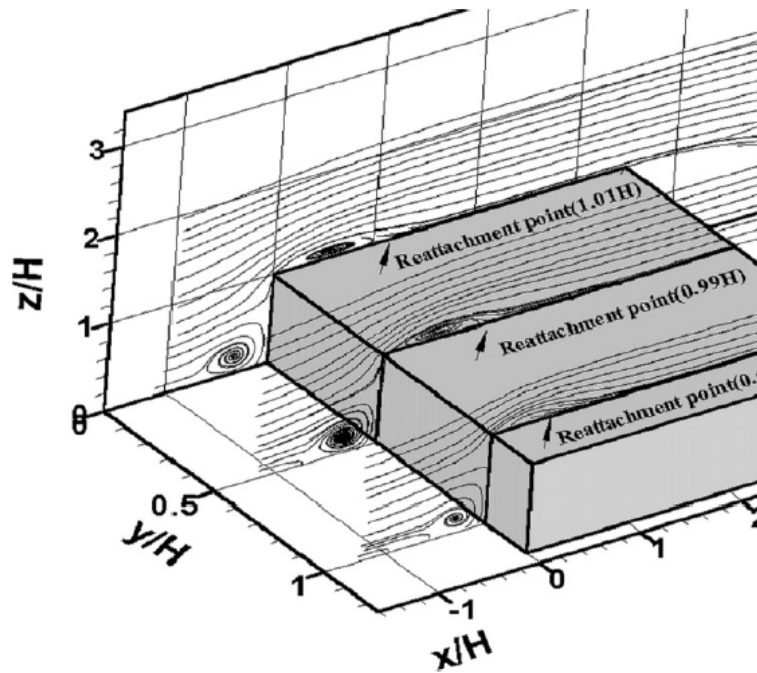


Figure 2.5: Velocity Profile through Canopy ($x/b=0$ to $x/b = 18$) (Coceal, 2003)



(a) Prism image including the three measurement planes.



(b) Streamlines at each measurement plane including separation/reattachment points.

Figure 2.6: Prism Figures from Kim et al. (2003)

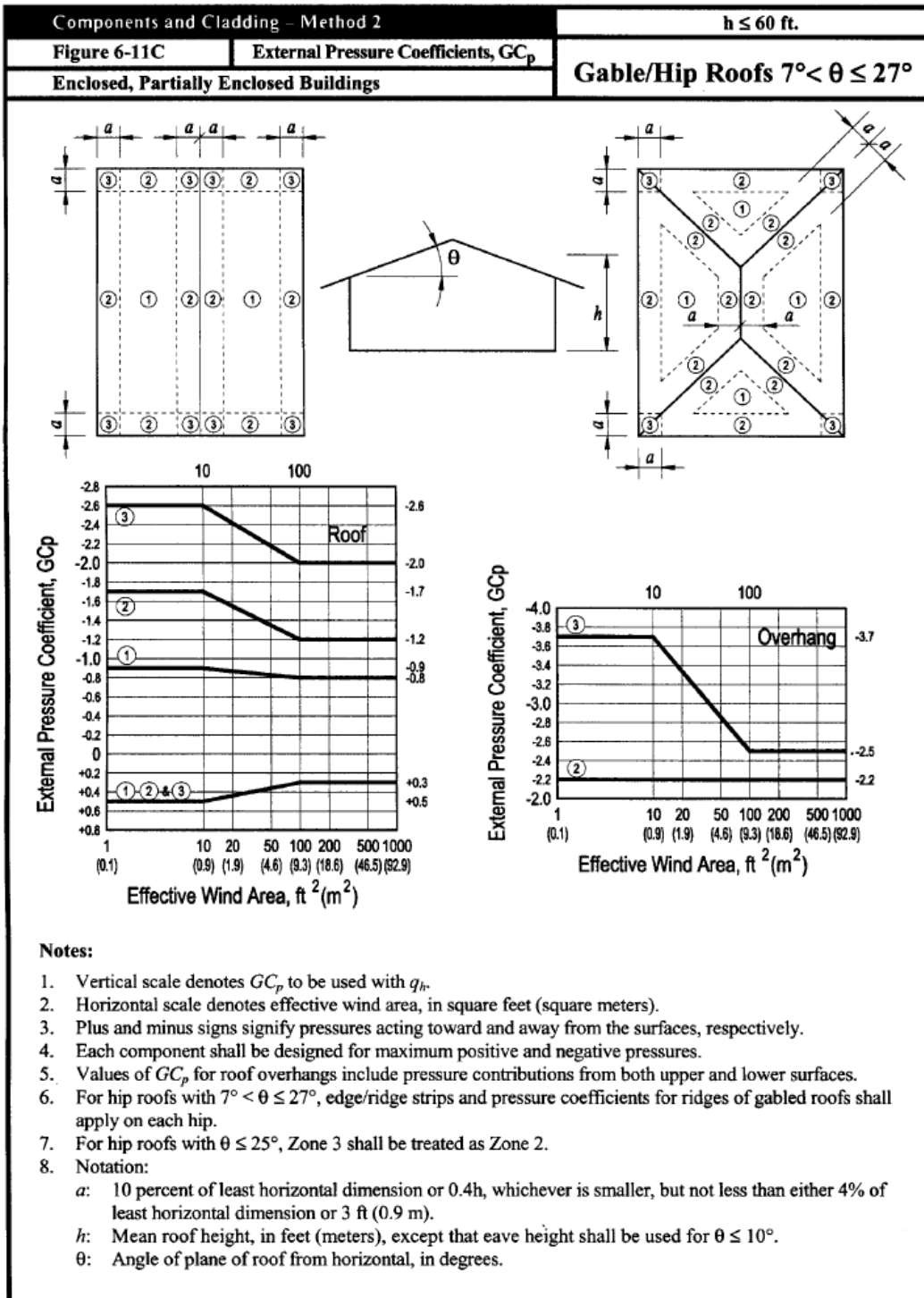


Figure 2.7: Wind pressure coefficients for a gable/hip roof system (ASCE 7-05)

3.0 LIFE CYCLE ASSESSMENT OF AEH

The objective of this chapter is to assess the environmental impacts of the AEH being developed by Dr. Lisa Weiland, Dr. Dan Cole, and Tim Bagatti (see Section 1.2.3), from raw material extraction to manufacture. These impacts will be reported according to ISO 14040 standards summarized in Chapter 2, allowing the results to be compared to other studies regarding manufacturing impacts of small-scale energy technologies. However, no comparison to other AEHs will be presented as there are no life cycle studies available in the literature and many of the competing technologies are proprietary to some degree. These initial results are not intended to provide a final conclusion about the impacts of the AEH; they are intended to be used to compare alternative material selections for the AEH and to help guide the improvement of the design from a manufacturing standpoint. In order to study the results of the alternative material choices, a decision matrix has been created and each material choice has been rated based on multiple variables. This will allow for material options to be selected based on the importance of any one of the chosen variables.

3.1 GOAL AND SCOPE

3.1.1 Objective and Scope

The aim of this chapter is to determine the environmental impacts of producing a single AEH in its current *prototype* form, focusing especially on the energy requirements of AEH production. Since this AEH is only a prototype built to be tested in a controlled environment, LCA will be used to study alternative materials which are aimed at reducing the energy requirements of production. Since there are no other studies pertaining to LCA of AEHs, results of this LCA of the AEH prototype will provide a reference point for future studies as the prototype transforms into the consumer-ready product. The material combination with the least environmental impact (especially energy requirements) will be determined.

3.1.2 Functional Unit

In order to provide results that allow for a *post priori* comparative study of other small-scale energy producing technologies, the functional unit will be defined as 1 kWh of electricity produced.

3.2 LIFE CYCLE INVENTORY

The data collected on the specifications of the AEH has come from either Dr. Wieland's specifications or calculating mass based on the material's specific properties. The software program SimaPro v.7 (Pre Consultants, 2007) has been used for this study to assist in performing the LCA. The following databases included in SimaPro were used for creating the AEH model: ETH-ESU 96, Ecoinvent v. 1.2, and Industry Data 2.0.

3.2.1 Current AEH Materials

The three primary parts of the AEH (Figure 1.6) are 1) the frame, 2) the coil/magnet apparatus, and 3) the belt. Currently the frame is built out of two sheets of acrylic, two lengths of 6105-T5 aluminum beams, and one length of PVC pipe used to keep the belt taut. Each coil/magnet apparatus is made of a length of copper wire spun into a cylinder. The magnets are rare earth magnets, consisting of metals such as neodymium and boron. The belt is made of a taffeta tape, similar to kite material.

3.2.2 System Boundaries

The life cycle was divided into four primary stages: 1) raw materials acquisition (upstream processes), 2) production of the AEH (manufacturing stage), 3) utilizing the AEH (use phase), and 4) final disassembly and disposal (end-of-life). Figure 3.1 shows the activities involved in the life cycle of an AEH. The dashed items are not included in this study. Since the AEH is only

in the prototype stage, this LCA will be a cradle-to-gate study, addressing only the first two stages.

The first stage includes the activities required to gather and manufacture the needed materials of the AEH. These include mining for copper, bauxite extraction to produce the aluminum beams, or mixing various chemicals to produce acrylic plastics. Transportation of the aluminum beams from Columbus City, Indiana to Pittsburgh, Pennsylvania is included. However, transportation of the remaining materials is omitted as information about the material origins is unknown. Since the AEH only weighs approximately 10 kg, transporting materials will not have a large impact on this study; however, this must be included in future studies to properly address large-scale manufacturing of the AEH.

The manufacturing stage is when the actual AEH is assembled. For this prototype, the belt has been assembled by hand using simple tools, which will be included in this study, but produce no impacts. For larger-scale production, automated production of the AEH components is anticipated. Due to the need to ‘tune’ the belt, manual final assembly may still be necessary. Compared to HAWTs and VAWTs, assembly should be much less energy intensive as the AEH contains no moving parts, as opposed to other types of wind energy generators.

The use phase is the operation of the AEH. While this phase will be omitted in the LCA, the potential energy outputs from Chapter 4 in this study will be used in determining energy payback time.

The final phase of the AEH is decommissioning and disposal. With no AEHs in operation, information about this phase is not addressed.

3.2.3 Alternative Material Options

The current version of the AEH was built for rapid prototyping and controlled testing, not long-term outdoor use. As a result, some of the material choices will not be suitable for permanent installation. This study will perform a sensitivity analysis and create a decision matrix, focusing on alternative materials for the frame of the AEH. Choosing different materials for the magnet/coil combination would likely reduce the output of the AEH as neodymium-boron magnets are one of, if not, the strongest magnets available for this type of application. Other materials such as gold and silver are better conductors of electricity, but due to the large amount of wire needed and the price premium of gold and silver, copper is the most realistic choice for the AEH. As stated previously, the taffeta tape belt used in testing will not be the material used in the final AEH design and with research still at an early stage, speculating on alternative materials is premature.

The frame currently consists of acrylic sheets, aluminum beams, and PVC pipe. The aluminum beams have been modeled assuming 100% virgin material. The first alternative explored uses 100% recycled aluminum beams. A third option is to use steel beams. Finally, a wood option is explored. This latter option may not be suitable for highly industrialized areas, but may prove suitable in developing areas and countries. The acrylic sheets are the ‘walls’ of the AEH (Figure 1.6). This material is not suitable for long term outdoor use, and alternatives must be explored. Similar to the beams, three options will be considered: aluminum (100% recycled), steel, and plywood. The prototype uses a PVC pipe, cut to resemble an open channel, which aids in keeping the belt taut during use. This also will not hold up under outdoor conditions. Different options for this pipe include using a steel or aluminum pipe in a similar

fashion as well as assuming the need for this pipe is eliminated through the development of the AEH.

3.3 RESULTS OF LIFE CYCLE IMPACT ASSESSMENT

The Life Cycle Impact Assessment (LCIA), which is the step in LCA which quantifies the environmental impacts, was performed for the entire extraction and manufacturing stages of the prototype AEH life cycle. Within SimaPro, the LCIA tool titled “Tool for the Reduction and Assessment of Chemical and Other Environmental Impacts” (US EPA, 2009), or TRACI was used to calculate the environmental impacts presented in this section. For example, Global Warming Potential (GWP) is measured in units of CO_{2eq}. Any pollutant that is considered to contribute to Global Warming will have an equivalency factor, or potential. Methane, for instance, has a GWP of 21 kg CO_{2eq} per kg of methane. That is, for each kg of methane emitted into the environment, the LCIA tool would record it as 21 kg of CO_{2eq} emitted. This creates a common unit to sum the many chemicals and compounds contributing to this impact category.

3.3.1 Energy Consumption

The energy consumption for the cradle to gate life cycle of a single AEH in its current form is approximately 1,257 MJ, or 349 kWh. The majority of the energy requirements (85%) are a result of the aluminum and acrylic parts of the AEH. The aluminum beams require 238 MJ/kg,

which is at the upper bound of life cycle energy requirements calculated by the International Aluminum Institute (2003) (93.7 – 238.9 MJ/kg). While acrylic will not be a final material choice for the AEH, it provides a reference point for energy consumption and materials should be chosen that will require less energy than the acrylic sheets.

3.3.2 Environmental Impacts and Energy Payback Period

In addition to energy consumption, Table 3.1 presents results of four selected impact categories, Global Warming Potential (GWP), Smog, Respiratory Effects, and Ozone Depletion. For three of the four categories (excluding Respiratory Effects), the production of the virgin aluminum and the acrylic sheets accounted for at least 85% of the impacts. It is clear that alternatives to these two materials making up much of the frame's mass, energy requirements, and environmental impacts, need to be explored as the prototype is improved upon.

The energy payback period is calculated by dividing the life cycle energy requirements by the average annual electricity productions of 0.1, 0.5, and 1 kWh. Detailed steps as to how these outputs were calculated can be found in Chapter 4. With the production of the current AEH requiring 349 kWh of electricity, even the greatest AEH output would require hundreds of years to offset this amount. This was expected due to the high energy requirements of the materials used and that the technology is still in its prototype stages, resulting in materials that have not been optimized as well as very conservative production estimates. In order to reduce this payback period, the output of the AEH needs to improve by roughly one order of magnitude (believed to be achievable) or the energy requirements of the AEH needs to decrease by roughly

one order of magnitude (achievable through mass production and/or less energy intensive material options).

3.3.3 Comparison with Other Energy Methods

Since the functional unit has been chosen as kWh, the environmental impacts and energy requirements can be compared with other energy sources. While sources such as coal and natural gas can be compared with this technology, they are not in the same energy market as the AEH, which is designed to produce small amounts of electricity. For this study, the environmental impacts and energy requirements will be compared to other wind turbines and solar power. These two options are often installed in the same settings as the AEH will be.

Rankine et al. (2006) found that for a 1.5 kW small-scale wind turbine, the CO₂ emissions ranged from 20.7 g/kWh to 121.4 g/kWh and the corresponding energy requirements ranged from 0.195 MJ/kWh to 1.14 MJ/kWh, based on the output of the turbine. The latter value is the amount of energy required in turbine production per kWh of electricity produced by the turbine. The current AEH has an energy requirement range of 62.85 MJ/kWh to 628.5 MJ/kWh, using lifetime outputs of 2, 10, and 20 kWh. The CO₂ emissions range from 4.1 kg/kWh to 41.2 kg/kWh. These values for the AEH are much higher, but again, this is comparing commercialized turbines to a prototype. Reducing these values by an order of magnitude or more would put them in the same range as the 1.5 kW small-scale turbine.

Solar panels are often installed on the roofs of buildings and can be used in place of or as a complement to small-scale wind power. Hondo (2005), in addition to studying emissions of large-scale wind turbines, produced life cycle emission results of solar panels as well. After

converting the results to reflect a 20 year lifetime (the study used 30 years), the CO₂ emissions of a 3 kW photovoltaic system are 71 g/kWh, which is similar to emissions of the 1.5 kW wind turbine.

3.4 SENSITIVITY ANALYSIS

In this section, the alternative material options for each section of the frame were modeled. In each case, all other parts of the frame were modeled as the original AEH, allowing each part to be isolated and analyzed. The same LCIA tool TRACI was used as in Section 3.3.

3.4.1 Energy Consumption

Table 3.1 shows the energy consumption for each alternative. Using recycled aluminum to replace the virgin aluminum or acrylic sheets reduces the energy requirements of the AEH's production by 35%. This is because 100% recycled aluminum can reduce the energy requirements of production by 90% compared to virgin aluminum. Steel beams also result in reduced energy consumption, but it must be kept in mind that steel beams are much heavier than aluminum, which could create difficulties during installation. The wood 'beam' alternative requires the least amount of energy in production, but the strength and durability of this AEH version will be significantly less than aluminum or steel versions.

In regards to the PVC pipe, it should either be kept in its current form or removed from the prototype. Producing the small amount of PVC required for the AEH takes very little energy,

as the overall energy consumption only dropped 5 kWh (2%) when the pipe was removed. Aluminum and steel pipes are both much heavier and increase the energy requirements of the AEH production and should not be used in this case.

3.4.2 Environmental Impacts and Energy Payback Period

With many choices for alternative materials, a decision matrix has been created to aid in selecting a material combination that minimizes environmental impacts. This matrix is shown in Table 3.2. Each of the original materials was assigned a value of 1. For each of the categories (energy consumption, weight, etc.), the alternative material choices were assigned values relative to 1. For example, considering the weight of the AEH, since steel is approximately 3 times heavier than aluminum, the steel beam replacement of the aluminum beam would be assigned a value of 3 while the aluminum beam value is 1. Each of the 9 categories was considered to carry equal weight in the matrix.

For each of the three portions of the frame, the material with the lowest score from the decision matrix was chosen and modeled. These three choices were 100% recycled beams instead of virgin aluminum beams, 100% recycled aluminum sheets instead of acrylic, and the no pipe option relating to the PVC pipe. In addition to creating a model based on the decision matrix, using values from the impact categories shown in Table 3.1 allowed for a model to be created that minimized the environmental impacts, omitting other variables such as cost, strength, and weight. This resulted in an AEH model with wooden 2 x 4s, plywood sheets, and no pipe to replace the original aluminum beams, acrylic sheets, and PVC pipe in the prototype.

As shown in Figure 3.4, the decision matrix model significantly reduced the environmental impacts and energy consumption. The energy consumption was reduced from 349 kWh to 92 kWh, a 75% reduction, and each of the four impact categories also showed reductions compared to the original model. The materials chosen to minimize environmental impacts showed even greater reductions, including a 90% reduction in energy consumption and GWP. However, both the wood 2 x 4s and plywood sheets were used in this model, and the AEH is unlikely to be built for urban use with these choices.

Table 3.1 shows substituting wooden 2 x 4s for the aluminum beams and making no other alterations, reduces the energy consumption by 50%. Still assuming a 1 kWh annual production with a 20 year life span, the energy payback time would not be within the 20 year life of the AEH. The decision matrix model and minimum impact model reduce energy consumption even more, but the payback still is greater than 20 years in both cases.

The two variables involved in energy payback are the AEH energy output and the energy requirements of producing and manufacturing the AEH. The decision matrix has allowed for changing the energy consumption, while the AEH output has remained constant. While the belt is still in very early development, it can be assumed that the output will be improved by the time the final version of the AEH is completed. Table 3.3 summarizes the AEH's annual energy production needed to equal the energy requirements of producing the AEH. This 'break-even' point is shown for five selected payback periods. Currently, the calculated annual output found in Chapter 4 will not satisfy any of these requirements. Keeping in mind this is still in the development stage, either an increase of AEH output or decreasing energy requirements an order of magnitude would potentially make the AEH viable from an energy payback standpoint. Both

of these options are very real possibilities and achieving both would certainly result in the AEH producing more energy than what would be required for its production.

3.4.3 Comparison with Other Energy Methods

The decision matrix AEH model as well as the option which minimized environmental impacts both resulted in reduced energy consumption and CO₂ emissions. Keeping the same three outputs of 2, 10, 20 kWh, the per kWh energy requirement ranges reduce to 4.6 – 46 MJ/kWh and 1.9 – 19 MJ/kWh for the decision matrix model and minimal environmental impact model, respectively. The same ranges drop to 0.99 – 9.9 kg/kWh and 0.31 – 3.1 kg/kWh for CO₂ emissions. These values still are very high compared to solar power and other small-scale wind turbines. As the development of the AEH continues, these numbers should continue to drop, with a goal of reaching the ranges of solar and small wind turbines. From an environmental perspective, these ranges must be reached to be considered a preferable alternative.

3.5 DISCUSSION OF RESULTS

It should be noted that the LCA presented has been conducted on a *prototype* AEH which is expected to improve as development continues. Thus, the analysis presented in this study should be interpreted as one approach to improving the viability of the AEH and the results should not be taken as ‘hard’ data. Furthermore, since the AEH is expected to be mounted on a building, much of the prototype’s frame may not be necessary as the substrate building will provide a

majority of the support. This will simplify the manufacturing process by reducing the amount of material required and in turn, mitigate many of the impacts reported in this study.

There are a number of conclusions that can be taken from the use of LCA techniques in modeling environmental impacts of this AEH prototype and utilizing LCA to study alternative material options in order to reduce these impacts, aiding in the development and viability determination of this technology:

1. The current AEH model requires a large amount of energy to manufacture and does not produce enough energy to ‘payback’ the production energy requirements inside the 20 year assumed lifetime.
2. Using wood as a material choice for the frame significantly reduces the environmental impacts and energy consumption during AEH production. However, wood is much weaker and less durable than steel or aluminum, which is less conducive to installing these AEHs on the roofs of large office buildings.
3. 100% recycled aluminum should prove to be a good choice from an LCA perspective, as it requires much less energy to produce as virgin aluminum, is approximately 1/3 the weight of steel, and is much stronger than wood.
4. Increasing the AEH output by an order of magnitude and reducing the energy consumption and environmental impacts by an order of magnitude should result in the AEH being determined viable for production and use. Both of these improvements are not unreasonable goals.

Table 3.1: Impacts due to AEH production: current version and alternatives

	Energy Consumption (kWh)	GWP (kg CO _{2eq})	Smog (kg Nox _{eq})	Respiratory Effects (kg PM2.5 _{eq})	Ozone Depletion (kg CFC-11 _{eq})
Original Model	349	82.35	0.14	0.058	2.01E-05
<u>Beam Alternatives</u>					
100% Rec. Al. Beams	225	49.07	0.09	0.056	2.21E-06
Steel Beams	292	64.63	0.12	0.099	2.53E-06
Wood (2 x 4s)	168	40.20	0.10	0.048	8.26E-07
<u>Acrylic Alternatives</u>					
100% Rec. Al Sheets	226	62.20	0.10	0.031	2.36E-05
Steel Sheets	247	60.3	0.10	0.053	2.05E-05
Plywood Sheets	213	47.13	0.09	0.031	2.01E-05
<u>Pipe Alternatives</u>					
100 % Rec. Al. Pipe	371	103.77	0.18	0.059	2.77E-05
Steel Pipe	416	99.67	0.18	0.109	2.09E-05
No Pipe	344	81.46	0.14	0.058	2.01E-05

Table 3.2: Decision Matrix for alternative material options

Category:	GWP	Energy Consumption	Smog	Respiratory Effects	Ozone Depletion	Lifetime	Strength	Cost	Weight	Unbiased Total
Virgin Al. Beams*	1	1	1	1	1	1	1	1	1	9
Recycled Al. Beams	0.6	0.64	0.64	0.97	0.11	1	1	1	1	6.96
Steel Beams	0.78	0.84	0.86	1.71	0.13	1	1	1.5	3	10.82
Wood 'Beams'	0.49	0.65	0.71	0.83	0.04	3	3	0.6	2	11.32
Acrylic Sheets*	1	1	1	1	1	1	1	1	1	9
Recycled Al. Sheets	0.76	0.65	0.71	0.53	1.17	1	0.5	2	0.5	7.82
Steel Sheets	0.73	0.71	0.71	0.91	1.02	1	0.5	2	1.5	9.08
Plywood Sheets	0.57	0.61	0.64	0.53	1	3	1	1	0.75	9.1
PVC Pipe*	1	1	1	1	1	1	1	1	1	9
Recycled Al. Pipe	1.26	1.06	1.29	1.02	1.38	0.5	0.5	2	5	14.01
Steel Pipe	1.21	1.19	1.29	1.88	1.04	0.5	0.5	2	5	14.61
No Pipe	0.99	0.99	1	1	1	0	0	0	0	4.98
* Original material										

Table 3.3: Required AEH Outputs for Selected Payback Periods

Energy Payback Period (years)	Annual Output Required (kWh)		
	Prototype	D.M.	Min. Imp.
1	349.0	92.0	37.0
5	69.8	18.4	7.4
10	34.9	9.2	3.7
15	23.3	6.1	2.5
20	17.5	4.6	1.9
D.M = Decision Matrix Option, Min. Imp. = Minimum Impact Option			

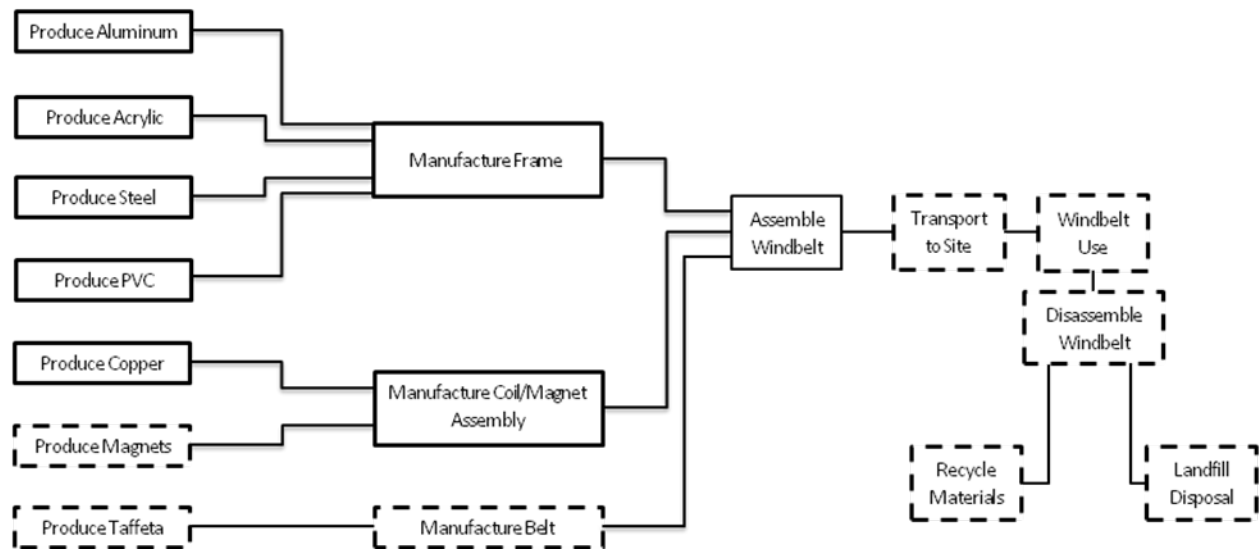


Figure 3.1: AEH flowchart (dashed boxes are outside the system boundaries)

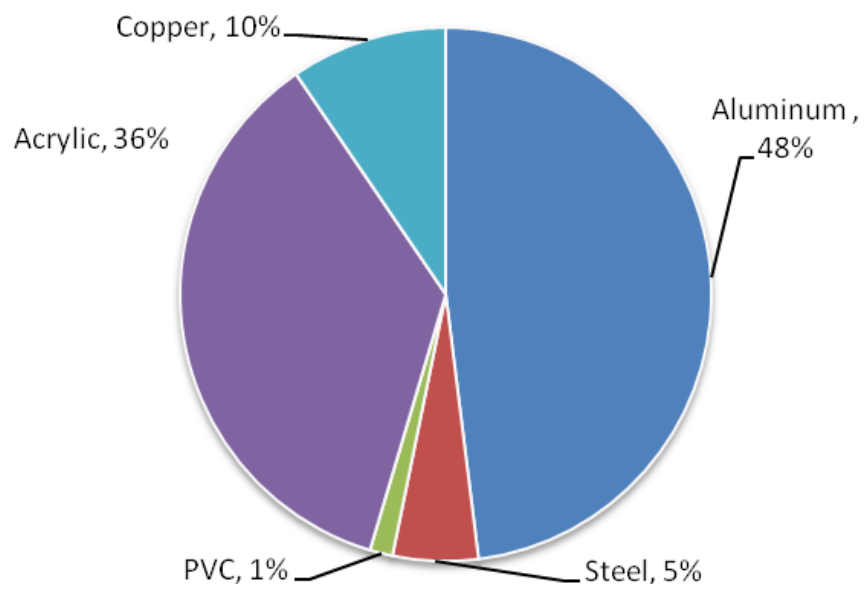
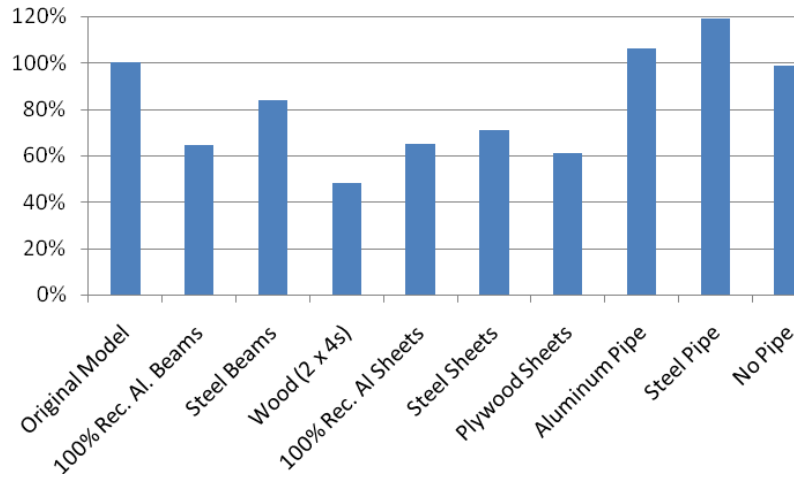
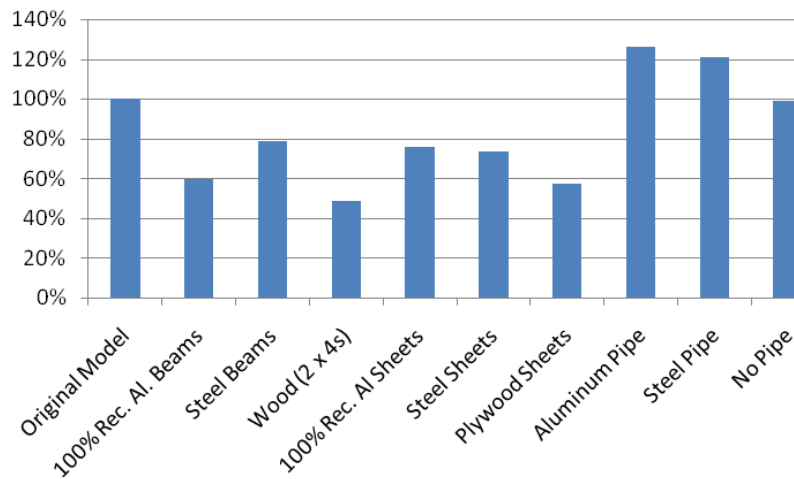


Figure 3.2: Percentage share of energy consumption of primary AEH materials



(a) Normalized Energy Consumption for each alternative material



(b) Normalized GWP for each alternative material

Figure 3.3: Normalized results for energy consumption and GWP

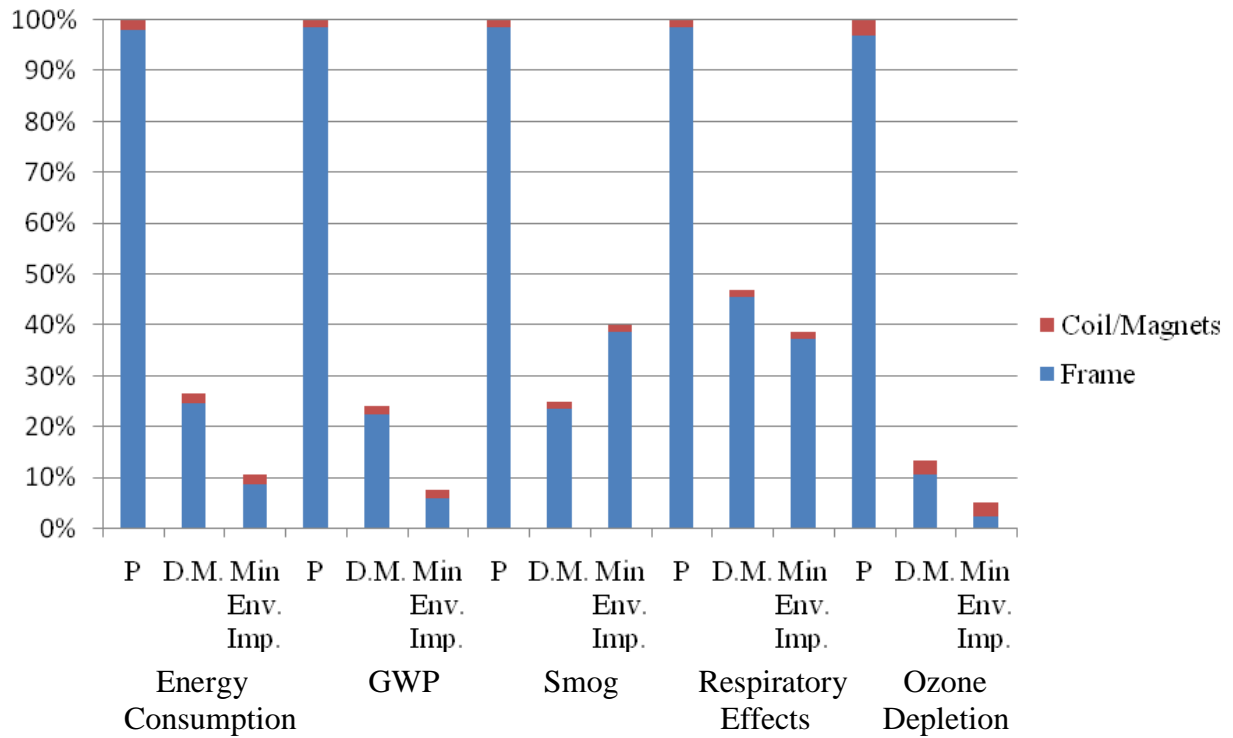


Figure 3.4: Normalized Impacts of Prototype, Decision Matrix, and Minimum Environmental Impact options

4.0 LOCAL WIND ENERGY GENERATION IN AN URBAN ENVIRONMENT

The objective of this chapter is to assess the potential for small-scale wind energy generation in an urban environment. The following discussion is premised upon some of the fundamental conclusions of Chapter 2 as described in Section 2.5. For this study, the city of Pittsburgh, PA is used as a case study location. The steps required to carry out the assessment, described in Section 4.3, are not site specific and can be utilized for any urban location.

4.1 WIND ENERGY POTENTIAL IN PENNSYLVANIA

As discussed earlier, the wind energy potential of a location can be determined through Wind Power Density maps, which provide a wind power class, ranging from 1 to 7. The state of Pennsylvania consists of primarily classes 1 and 2, with a very small percentage represented by class 3 primarily along the Laurel Ridge and Erie shore (Figure 4.1). It is generally felt that class 3 locations are the lowest in which large-scale wind farms may be effectively sited; thus Pennsylvania is not well suited to large-scale wind energy generation. Nonetheless, a number of sites in Pennsylvania have been exploited and a strong local industry focused on manufacturing large-scale wind turbines has emerged.

4.2 PITTSBURGH DATA COLLECTION AND ANALYSIS

For this study, Pittsburgh, PA, has been selected as the urban environment considered. Data from this region will be used in the following sections. The data consists of instantaneous wind speed and directional measurements taken at least once per hour from January 2005 through December 2008 at the Pittsburgh International Airport (NCDC, 2009). This location can be classified as an ‘open field’, which means there are not any tall bodies to disrupt the wind flow in the area. The Pittsburgh airport is located approximately 9.6 km (6 miles) WNW of the Pittsburgh downtown area as shown in Figure 4.2. Wind speed measurements were taken at a standard height of 10 m above the ground surface and are reported in miles per hour (mph). Wind directional values were reported in ten degree increments, with 0 degrees being true north. The data was exported from the NCDC site into Microsoft Excel for organization and analysis. The wind speed measurements were converted from mph to meters per second (m/s). Since the data was taken in (typically) hourly increments it is assumed to represent an appropriately random sample of what may be considered ‘service-level’ wind loads. This is appropriate as this study is not focusing on design level wind events; the actual local wind environment (service level winds) is of more importance.

For this study, the wind directions were grouped into 16 segments around the compass (N, NW, NE, NNE, etc.) corresponding to directions used in weather forecasting. Using the software program WRPLOT View (Lakes Environmental, 2009), the four years of data was analyzed for directional frequency and wind speed range, producing the wind rose and distribution shown in Figure 4.3. A total of 40,647 data points were collected over the four years. In addition to the information provided by the wind rose, the mean wind speed and standard

deviation for each wind direction range were calculated. As seen in Figure 4.3 and Table 4.1, wind in the Pittsburgh area primarily blows from the west. In general, these winds also have larger average speeds than winds coming from other directions. For this study, seasonal variation was not considered; thus the data is considered only on an annual basis. It is feasible and may be advisable to consider such wind data on a seasonal basis since this will correlate with the electricity demand. It is theoretically possible to consider the hourly demands to further refine the analysis.

4.3 PITTSBURGH WIND ENVIRONMENT

4.3.1 Step 1: Open Field Wind Profile

For this study, the open field wind profile for downtown Pittsburgh (the so called ‘Point’ at the confluence of the Monongahela and Allegheny Rivers shown in Figure 4.4) was created based on the values found for the wind blowing from the W, WNW, and WSW directions ($W \pm 33.75^\circ$) which accounted for 31% of the frequency values. The reason for including these three directions is because initial tests on the AEH show it operates well in up to a 30° incident flow (Bagatti, 2009).

At an elevation of 10 m, the average speed is 4.1 m/s with a standard deviation of 2.8 m/s. Since wind power classes are determined based on wind speeds at an elevation of 50 m, the power law (Equation 2.1) with $\alpha = 0.14$ was used to determine the 50 m west wind speed. At 50 m, the wind speed increased to 5.1 m/s, a 25% increase, and places the location just below wind

power Class 2 (Marginal). Considering a range of wind speeds represented by one standard deviation (68% confidence interval) and assuming the standard deviation varies linearly with the mean, the range of expected wind speeds at an open field elevation of 50 m is 1.6 – 8.6 m/s (see Table 4.2). The winds blowing from the East are not considered since a) they blow at much lower speeds and less frequently; and b) downtown Pittsburgh is sheltered by hills (the Hill District) to the east. It will be assumed the AEHs will be installed in a N-S direction, allowing the belt to operate when winds blow from the West.

4.3.2 Step 2: Change of roughness into urban location

The downtown district of Pittsburgh is bounded by the Allegheny and Monongahela rivers to the North and South respectively (Figure 4.4) (all Google Map plan views in Figures 4.4 to 4.6 are oriented with North at the top). To the Northeast, these rivers meet to form the Ohio River. As seen in Figure 4.4b, the city has a distinct Western exposure and an abrupt change in roughness as the wind blows in from the west, over the rivers and into the downtown core. For this study, downtown Pittsburgh has been divided into 2 primary sections: buildings located along the rivers, and interior buildings, which are more centralized in the downtown area.

Two buildings, the Pittsburgh Hilton and the Westinghouse Tower, have been selected as representative perimeter buildings for this study. The Hilton (Figure 4.5a and b) is approximately 100 meters tall with a building footprint of 100 m x 15 m, with the long side essentially facing West. The Westinghouse Tower (Figure 4.5c and d) is 108 meters tall and has a building footprint of 28 m x 60 m, with the short side facing WNW. Figure 2.5 shows that as an open field wind flow approaches an urban district, the wind velocity at the edge of the district is

approximately 80% of the free field velocity. This will reduce the average velocity at 50 m elevation to 4.1 m/s and the range corresponding to one standard deviation to 1.3 – 6.9 m/s

The representative interior buildings selected are the U.S. Steel Tower (Figure 4.6a and b) and the FHL Bank Building (Figure 4.6c and d), both located on Grant Street. The iconic U.S. Steel Tower, the tallest building in Pittsburgh at 250 meters tall, has an isosceles triangular building footprint with sides of 80 m and 120 m. In Figure 4.6b, the 80 m sides intersect to point in the NW direction. The FHL Bank Building was chosen because it is shorter than 200 meters tall, which allows equations 2.4 and 2.5 to be used. These equations represent an alternative method of describing the flow in an urban area, which is described in Mertens (2003). It is 70 meters tall and has a building footprint of 30 m x 40 m, with the 40 m side facing WNW.

For interior buildings, the wind is much harder to predict as many variables affect the direction, speed, and turbulence. Nonetheless, the wind profile is still logarithmic in nature. However, the velocity is significantly reduced. Ricciardelli and Polimeno (2006) found through experimentation a 30% reduction from the free flow velocity while the urban canopy model developed by Coceal (2003) estimates a 45 – 50% reduction inside an urban district. For this study, it will be assumed the mean wind speed inside the city of Pittsburgh will be 40% less than the open field wind speed. Therefore, the velocity range at an elevation of 50 m will be 0.9 – 5.2 m/s. This will be referred to as Interior Method 1 and will be used for the U.S. Steel Tower only.

Utilizing equations 2.4 and 2.5, the height of the RS and a mean wind speed profile can be developed. The FHL Bank Building is approximately 1000 meters away from the change in roughness represented by the western exposure of downtown Pittsburgh. The roughness length used to equate the height of the RS at the tower is 10 m, which is in the middle of the range found in literature. Thus, the height of the RS is:

$$h(x) = 0.28 \times 10 \times \left(\frac{1000}{10} \right)^{0.8} = 112 \text{ m} \quad (2.4)$$

The wind speed at roof level is:

$$u(70) = \frac{\ln\left(\frac{h_1(1000)}{0.03}\right) \ln\left(\frac{70 - d_o}{10}\right)}{\ln\left(\frac{10}{0.03}\right) \ln\left(\frac{h_1(1000) - d_o}{10}\right)} u(10) = \frac{\ln\left(\frac{112}{0.03}\right) \ln\left(\frac{70 - 50}{10}\right)}{\ln\left(\frac{10}{0.03}\right) \ln\left(\frac{112 - 50}{10}\right)} 4.1 = 2.2 \text{ m/s} \quad (2.5)$$

This will be referred to as Interior Method 2, only used on the FHL Bank Building, producing a range of wind speeds at an elevation of 70 m (roof level of FHL) corresponding to one standard deviation of 0.7 – 3.8 m/s.

After calculating the wind speeds at 50 m elevation for the three buildings save the FHL building, the wind speed at each roof level was established by using the power law (Equation 2.1) with $\alpha = 0.14$. The resulting values are presented in Table 4.2.

4.3.3 Step 3: Flow around buildings/concentrator effects

The Pittsburgh Hilton has no obstructions in the windward direction. As the wind flows over and around the windward face, it should accelerate and create turbulence near the building surfaces, especially at the roof. According to Lu and Ip (2009), the wind speed should exhibit a 50 – 100% increase. This would create wind speed ranges of 2.2 – 11.4 m/s (50%) and 2.9 – 15.2 m/s (100%) as the wind flows past the building. These locations of increased turbulence are the optimal locations for installation of AEHs. For simplicity, the remaining calculations will only report a conservative 50% increase.

The Westinghouse Tower also has no large obstructions in the windward direction. However, the building geometry is different than the Hilton. While the Hilton has a primarily flat façade facing the west, the Westinghouse Tower has a recessed area around the building's perimeter approximately 50 m from the ground level (see Figure 4.5c). This area creates another potential location for AEH installation as recirculation bubbles form, causing increased turbulence and/or wind speed. With no research that discusses wind behavior in a recessed area of a building, it will be assumed the wind speed inside the area increases 50% just as the roof level speeds do, creating a range of 2.0 – 10.4 m/s. At the roof level of the tower, the wind speed range will be roughly the same as the Pittsburgh Hilton when applying the results of Lu and Ip (2009): 2.2 – 11.6 m/s (50%).

The U.S. Steel Tower is significantly taller than many of its surrounding buildings, which would generally reduce the acceleration of the wind speeds at the roof level. However, according to Lu and Ip (2009), the combination of concentrator effects and increased wind speed at higher elevations will still result in a 50 to 100% increase in wind speed. A 50% increase results in a range of 1.8 – 9.7 m/s.

For the FHL Bank Building, the acceleration around the building may not be as significant, due to the shorter height, decreased wind speed at lower elevations, and the protection offered by taller surrounding buildings. Based on the results from Lu and Ip (2009), the increase of wind speeds around a building surrounded by taller buildings should not be more than a 50% increase. This will result in a range of 1.1 – 5.6 m/s, significantly lower than the nearby U.S. Steel Tower.

A summary of wind speed predictions for each of the previous three steps taken for the four buildings can be found in Table 4.2.

4.3.4 Step 4: Apply current AEH output results

The current data on the prototype AEH output is that it will produce 50 mW of power at a wind speed of 2 m/s in smooth flow. Anecdotal observations indicate an improvement in performance when a) turbulence is present, and b) when the AEH is oriented vertically. For this study, the output of 50 mW at 2 m/s will be used as a benchmark for the following discussion. The AEH has a cut-in speed of 2 m/s, below which the AEH will not operate.

In order to provide a range of potential outputs, 4 power curves have been created. As Equation 2.8 shows, power is proportional to the cube of wind speed. This is an extreme upper-bound since it does not take into account the efficiency of the AEH. A simple relationship in Equation 4.1 allows multiple power curves to be created, based on values of k and n .

$$P = kV^n \quad (4.1)$$

Table 4.3 shows the k and n values used in constructing the four power curves, seen in Figure 4.7. In each case, k was selected to result in an output of 50 mW at 2 m/s. These curves are not intended to provide a performance curve for the AEH; instead, the multiple curves have been created to calculate a range of potential outputs since very little data is available concerning the AEH's energy production.

The AEHs should be positioned on the west side of the building to capture the most energy as the highest wind speeds come from the west. Since the AEH will operate in winds coming at an incident angle of up to 30° , the open field wind rose and frequency distribution from the airport has been presented in terms of wind speeds having incident angles of $236^\circ - 304^\circ$ (Figure 4.8).

According to Table 4.1, wind speeds from the WSW, W, and WNW directions account for 31% of all the wind data. It can be assumed that at the selected buildings, this distribution remains appropriate. Figure 4.8b shows the open field flow frequency distribution of the AEH operating range broken down into wind speed ranges. In order to use these values and distribution, each wind speed in the distribution must be ‘mapped’ to corresponding values for each building. This will transform the distribution speeds from an open field location at 10 m elevation to each individual urban area roof level. These values will be used with each of the power curves to estimate an AEH output. Table 4.4 shows these mapped values at each building’s respective height along with the corresponding frequency distribution. Calculating the energy output of an AEH follows the same procedure, no matter the building or power curve. The wind speed ranges from Table 4.2 are compared to each of the values from Table 4.4 and the wind speed ranges are used to calculate the power output based on the frequency at that wind speed. Calculations for each of the four buildings considered are shown in Tables 4.5 through 4.9.

Once the electric output for each relevant velocity has been calculated, they are summed together for each building. The result is the projected annual electricity production for one AEH at a specific location. For the Pittsburgh Hilton, one AEH installed on the roof is projected to produce 99, 646, 1294, and 5619 Wh of electricity annually for power curves 1 through 4, respectively.

While installing AEHs on the roof of the FHL Bank Building does not produce as much electricity as the other buildings, other alternatives are possible. The FHL Bank Building and the building across the street from it in the NW direction create a channel which is perpendicular to the wind flow. As Figure 2.4d shows, channels perpendicular to the wind direction create

recirculation regions along the sides of the buildings. These areas should have significant amounts of wind turbulence, which should increase the energy output of an AEH. With no data on energy output in a turbulent flow, projecting the output of an AEH in this area will not be done, but is a future step in the study of urban environment electricity production.

4.4 POTENTIAL USE OF AEH IN COMMERCIAL BUILDINGS

According to the 2003 Commercial Buildings Energy Consumption Survey (Energy Information Administration, 2006), office buildings annually consume approximately 186 kWh/m² of gross floor space and hotels consume 146 kWh/m². Useable floor area is estimated to be approximately 80% of gross floor space. The four buildings studied here, the Pittsburgh Hilton, Westinghouse Tower, U.S. Steel building, and FHL Bank building, have useable floor areas of approximately 26,400, 30,900, 214,000, and 17,300 m², respectively. Using these rates, the buildings should consume 4800, 7200, 49,800, and 4000 MWh/yr. For comparison, a single AEH on the roof of the FHL Bank Building based on Power Curve 3 will only produce 292 Wh (0.000292 MWh).

Figure 4.9 shows the hourly electric demand for a high-rise office building in Chicago, Illinois (US Environmental Protection Agency). The nighttime hours show a much lower demand, but the building has a minimum demand of approximately 150 kWh at all times. Assuming this demand is the only demand for 8 hours/day (i.e. 'off-peak hours'), a building would require 1200 kWh/day of electricity to meet this demand and 438,000 kWh/year. Using the Westinghouse Tower roof along with Power Curve 3 as an example, a single AEH would produce 1.3 kWh/year. In order to provide 1% of this minimum demand, there would need to be

3,370 AEHs installed on the roof, which is not feasible. According to these calculations, the AEH's electrical output must significantly increase if the goal of offsetting a building's electric demand is to be realized. Assuming 50 AEHs installed on the Westinghouse Tower roof, each AEH would need to produce 88 kWh/year in order to meet the 1% of the minimum demand, which would require a large increase in output from each AEH. These calculations are still very preliminary and will need to constantly be adjusted as more testing is completed on the AEH prototype. However, the current output of 50 mW at 2 m/s wind speed is considered well below the potential for this technology.

While these AEHs may not provide an alternative to grid electricity, they may prove to be appropriate for special applications including:

- Providing 'trickle' charging capability for battery operated systems in a structure
- Powering low demand systems, particularly those located on a building roof, such as clearance lighting or cellular and/or microwave repeater stations.

4.5 CONCLUSIONS ON PITTSBURGH WIND ENVIRONMENT

There are a number of conclusions that can be taken from the study of the Pittsburgh wind environment that will be beneficial in the future development and viability determination of micro and small-scale wind energy generating devices:

1. The four steps described in this study provide a foundation for analyzing wind energy potential in an urban environment. They are not specific to the AEH and can be used with any wind energy generator. However, these steps are unable to account for all the

variables affecting wind speeds inside very complex urban districts, which will reduce the accuracy of results. Complex computational fluid dynamics can theoretically provide improved guidance in this regard.

2. Buildings on the perimeter of an urban area should exhibit larger wind speeds flowing over and around the building as wind speeds will decrease further into the urban location, thus siting along coastlines appears to have greater potential.
3. Interior buildings that are very tall and have very few similarly tall buildings located in the immediate area should not be affected by the lower wind speeds in the city interior. Their height compared to the surrounding buildings will result in a relatively undisturbed wind speed at roof level.
4. Shorter buildings surrounded by buildings of similar heights will see the most significant reduction in wind speed from the free field values. In addition, the concentrator effect is minimized and the acceleration around the building may not be as significant as the perimeter and/or much taller buildings.
5. Since the AEH should operate more efficiently in turbulent wind regions, the shorter interior buildings should focus on the creation of vortices along streets (wind canyon and channeling effects) that are running perpendicular to the predominant wind flow direction.
6. The four power curves created provide a good preliminary range of potential power outputs of the AEH. More research is needed to assess the efficiency of the AEH outputs at different wind speeds.
7. Low operating speeds are essential in urban districts. For Pittsburgh, PA, 65% of the time, winds are below 5 m/s. A low operating speed of the AEH increases the amount of

operating time. From the literature review, Peacock (2008) showed that HAWT's in urban/suburban settings produce either no power or a fraction of their rated power a majority of the time (>90%) due to their higher cut-in speeds.

8. The AEH in its current state will not make a significant impact in a large office building's energy demands. While these results are still preliminary, they indicate the performance of AEH needs to improve by approximately an order of magnitude to potentially make an impact in an urban district. However, the primary goal of this AEH is not to significantly reduce large building energy demand. Instead, there are still specialized applications for the AEH that may prove feasible.
9. The approach reported in this chapter is not intended to yield final results but rather preliminary feasibility estimates. These could then be used to a) exclude a site from further consideration; or b) provide guidance for a more focused site assessment or more complex CFD analysis.

Table 4.1: Wind Data Summary at 10 m height

Direction	Degree Range	Avg. Speed (m/s)	Max Speed (m/s)	Std. Dev (m/s)	Frequency (%)	1 Std. Dev Range (m/s)
N	350-10	3.12	11.18	2.02	6.63	1.1 – 5.14
NNE	20-30	2.53	7.15	1.59	2.68	0.94 – 4.12
NE	40-50	2.655	10.28	1.74	2.52	0.91 – 4.39
ENE	60-70	2.64	7.60	1.74	2.76	0.9 – 4.38
E	80-100	2.65	9.83	1.68	4.74	0.97 – 4.33
ESE	110-120	3.09	10.73	2.0	3.85	1.09 – 5.09
SE	130-140	2.69	10.73	1.88	4.13	0.81 – 4.57
SSE	150-160	2.26	9.39	1.5	4.97	0.76 – 3.76
S	170-190	2.65	10.73	1.7	7.97	0.95 – 4.35
SSW	200-210	3.52	14.75	2.22	7.59	1.30 – 5.74
SW	220-230	3.42	17.43	2.23	8.48	1.19 – 5.65
WSW	240-250	3.26	14.75	2.16	9.39	1.10 – 5.42
W	260-280	4.21	16.99	2.91	14.98	1.30 – 7.12
WNW	290-300	4.81	17.43	3.21	6.89	1.60 – 8.02
NW	310-320	4.30	16.09	2.86	7.06	1.44 – 7.16
NNW	330-340	3.91	14.31	2.6	5.36	1.31 – 6.51

Table 4.2: Summary of wind speed values at roof levels

		Hilton			Westinghouse			US Steel			FHL Bank		
		x-σ	x	x+σ	x-σ	x	x+σ	x-σ	x	x+σ	x-σ	x	x+σ
Roof height	m	100			108			250			70		
Exposure		Perimeter			Perimeter			Interior			Interior		
Free field at 10 m	m/s	1.3	4.1	6.9	1.3	4.1	6.9	1.3	4.1	6.9	1.3	4.1	6.9
Free field at 50 m	m/s	1.6	5.1	8.6	1.6	5.1	8.6	1.6	5.1	8.6	1.6	5.1	8.6
Adjustments for Roughness													
City at 50 m	m/s	1.3	4.1	6.9	1.3	4.1	6.9	0.9	3.1	5.2	0.9	3.1	5.2
City at roof level	m/s	1.4	4.5	7.6	1.5	4.6	7.7	1.2	3.9	6.5	0.7	2.2	3.8
Concentrator Effect (conservatively assumed to be 150%)													
City at roof level	m/s	2.2	6.8	11.4	2.2	6.9	11.6	1.8	5.8	9.7	1.1	3.3	5.6

Table 4.3: Summary of k and n values in power curve creation

	k	n	Equation
Power Curve 1	25	1	$P = 25V^1$
Power Curve 2	17.7	1.5	$P = 17.7V^{1.5}$
Power Curve 3	12.5	2	$P = 12.5V^2$
Power Curve 4	6.25	3	$P = 6.25V^3$

Table 4.4: Wind speeds (m/s) used in AEH power calculations

		Corresponding building-specific speeds at AEH installation levels (m/s)				
Open Field Speed (m/s)	Frequency Distribution (%)	Hilton Roof	Westinghouse Roof	Westinghouse 50 m	USX Roof	FHL Roof
1	1.8	1.7	1.7	1.5	1.4	0.8
2	2.1	3.3	3.3	3.0	2.8	1.6
3	4.7	5.0	5.0	4.5	4.2	2.4
4	6.8	6.6	6.7	6.0	5.6	3.2
5	1.8	8.3	8.4	7.5	7.1	4.0
6	3.1	9.9	10.0	9.0	8.5	4.8
7	2.3	11.6	11.7	10.5	9.9	5.6
8	1.8	13.3	13.4	12.0	11.3	6.5

Table 4.5: Electricity outputs for a single AEH on Pittsburgh Hilton roof

Open Field Speed (m/s)	Hilton Roof	Frequency	Curve 1	Curve 2	Curve 3	Curve 4
1	1.7	0.018	7,884	7884	7,884	7,884
2	3.3	0.021	9,198	21,321	28,169	49,296
3	5.0	0.047	20,586	81,476	128,663	321,656
4	6.6	0.068	29,784	174,726	314,594	102,2429
5	8.3	0.018	7,884	69,164	142,405	605,220
6	9.9	0.031	13,578	151,998	339,450	1,697,250
7	11.6	0.023	10,074	139,076	333,072	1,915,162
Annual Total Output (mWh)			98,988	645,644	1,294,235	5,618,897
Annual Total Output (Wh)			99	646	1,294	5,619

Table 4.6: Electricity outputs for a single AEH on Westinghouse Tower roof

Open Field Speed (m/s)	Westinghouse Roof	Frequency	Curve 1	Curve 2	Curve 3	Curve 4
1	1.7	0.018	7,884	7,884	7,884	7,884
2	3.3	0.021	9,198	21,321	28,169	49,296
3	5.0	0.047	20,586	81,476	128,663	321,656
4	6.7	0.068	29,784	174,726	314,594	1,022,429
5	8.4	0.018	7,884	69,164	142,405	605,220
6	10.0	0.031	13,578	151,998	339,450	1,697,250
7	11.7	0.023	10,074	139,076	333,072	1,915,162
Annual Total Output (mWh)			98,988	645,644	1,294,235	5,618,897
Annual Total Output (Wh)			99	646	1,294	5,619

Table 4.7: Electricity outputs for a single AEH on Westinghouse Tower recessed area

Open Field Speed (m/s)	Westinghouse 50 m	Frequency	Curve 1	Curve 2	Curve 3	Curve 4
1	1.5	0.018	0	0	0	0
2	3.0	0.021	9,198	16,919	20,696	31,043
3	4.5	0.047	20,586	69,566	104,217	234,487
4	6.0	0.068	29,784	154,958	268,056	804,168
5	7.5	0.018	7,884	57,325	110,869	415,758
6	9.0	0.031	13,578	129,779	274,955	1,237,295
7	10.5	0.023	10,074	121,336	277,665	1,457,739
Annual Total Output (mWh)			91,104	549,881	1,056,456	4,180,491
Annual Total Output (Wh)			91	550	1,056	4,180

Table 4.8: Electricity outputs for a single AEH on U.S. Steel Building roof

Open Field Speed (m/s)	US Steel Roof	Frequency	Curve 1	Curve 2	Curve 3	Curve 4
1	1.4	0.018	0	0	0	0
2	2.8	0.021	9,198	16,919	20,696	31,043
3	4.2	0.047	20,586	58,300	82,344	164,688
4	5.6	0.068	29,784	135,997	225,242	619,414
5	7.1	0.018	7,884	51,689	96,579	338,027
6	8.5	0.031	13,578	119,115	245,253	1,042,324
7	9.9	0.023	10,074	112,773	251,850	1,259,250
Annual Total Output (mWh)			91,104	494,793	921,963	3,454,746
Annual Total Output (Wh)			91	495	922	3,455

Table 4.9: Electricity outputs for a single AEH on FHL Bank Building roof

Open Field Speed (m/s)	FHL Roof	Frequency	Curve 1	Curve 2	Curve 3	Curve 4
1	0.8	0.018	0	0	0	0
2	1.6	0.021	0	0	0	0
3	2.4	0.047	20,586	28,806	32,166	40,207
4	3.2	0.068	29,784	54,786	67,014	100,521
5	4.0	0.018	7,884	22,327	31,536	63,072
6	4.8	0.031	13,578	53,740	84,863	212,156
7	5.6	0.023	10,074	45,999	76,185	209,508
Annual Total Output (mWh)			81,906	205,658	291,763	625,464
Annual Total Output (Wh)			82	206	292	625

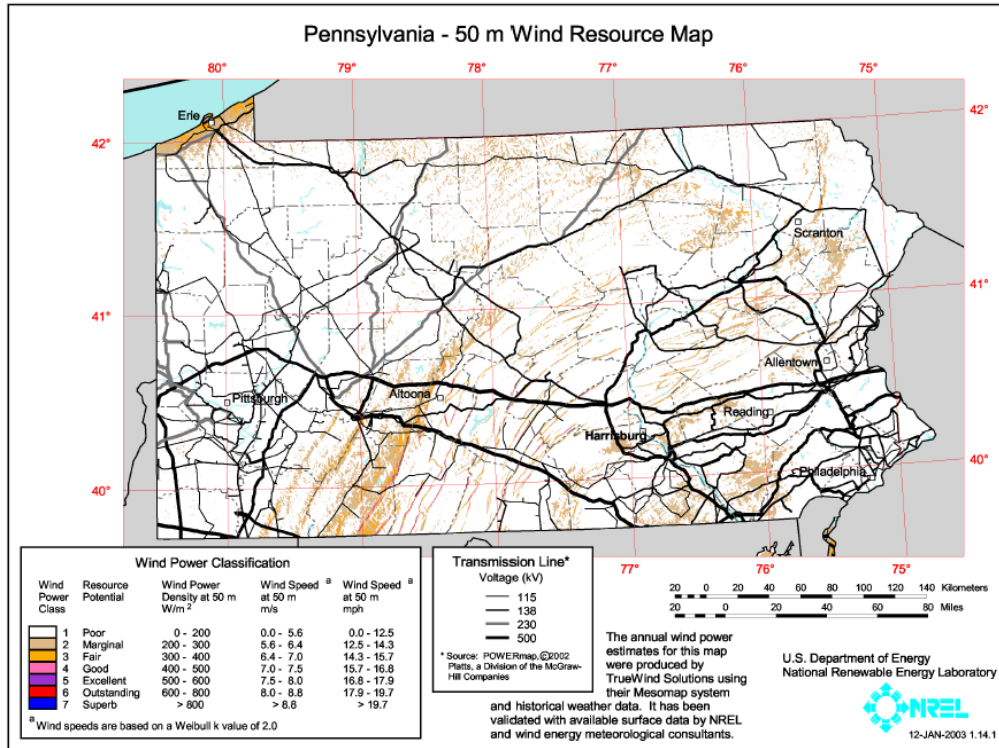


Figure 4.1: Pennsylvania Wind Power Map (US Department of Energy, 2009)

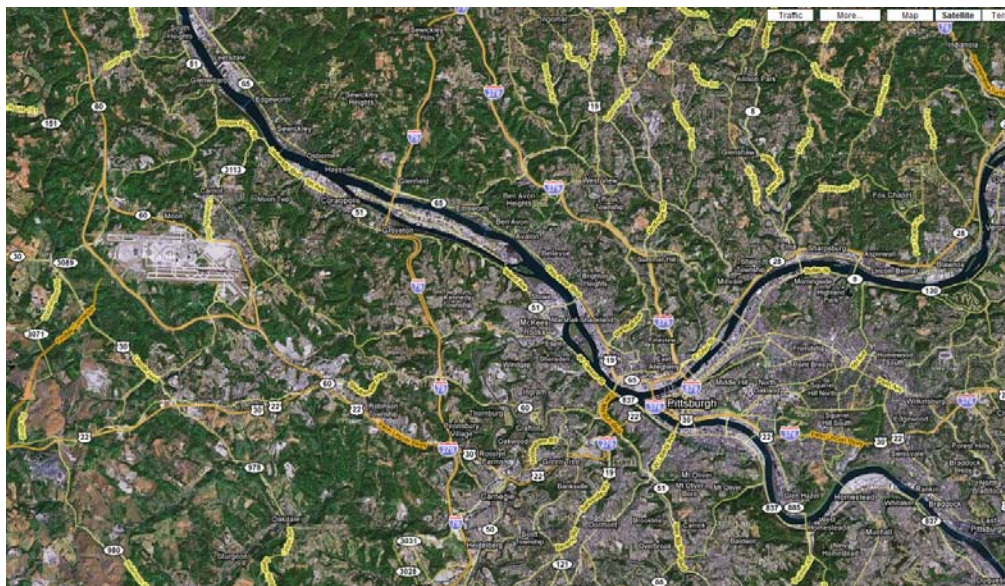
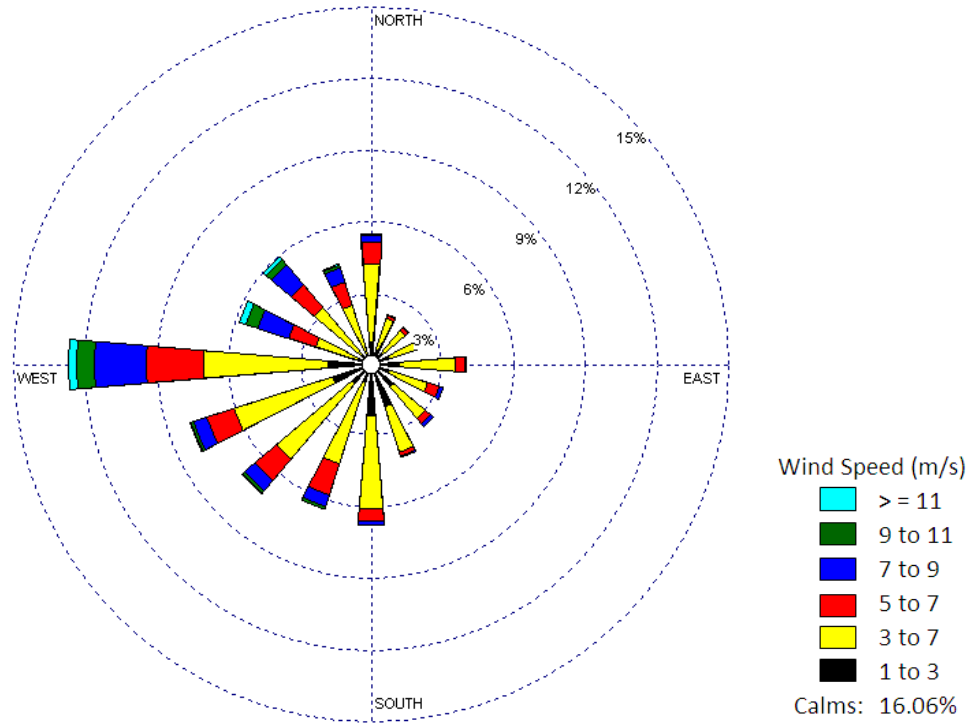
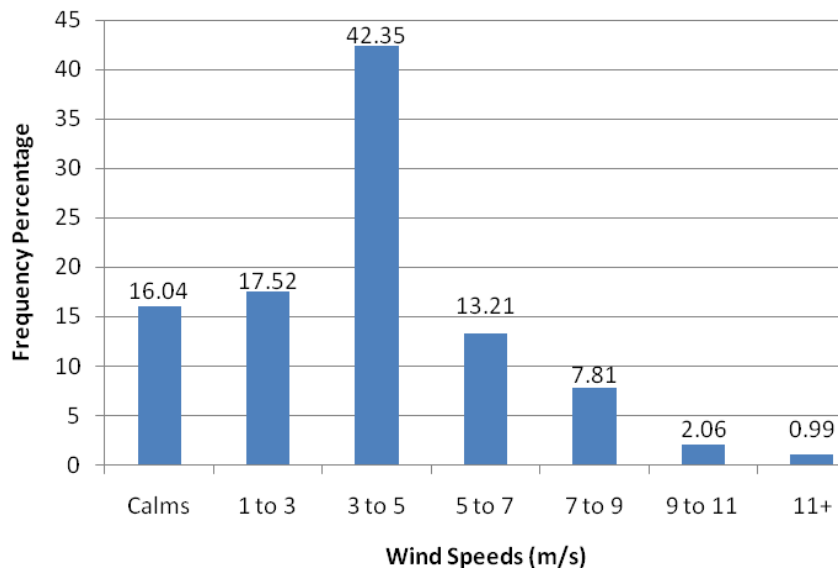


Figure 4.2: Pittsburgh Region showing downtown (center right) and airport (left) (Google Maps)

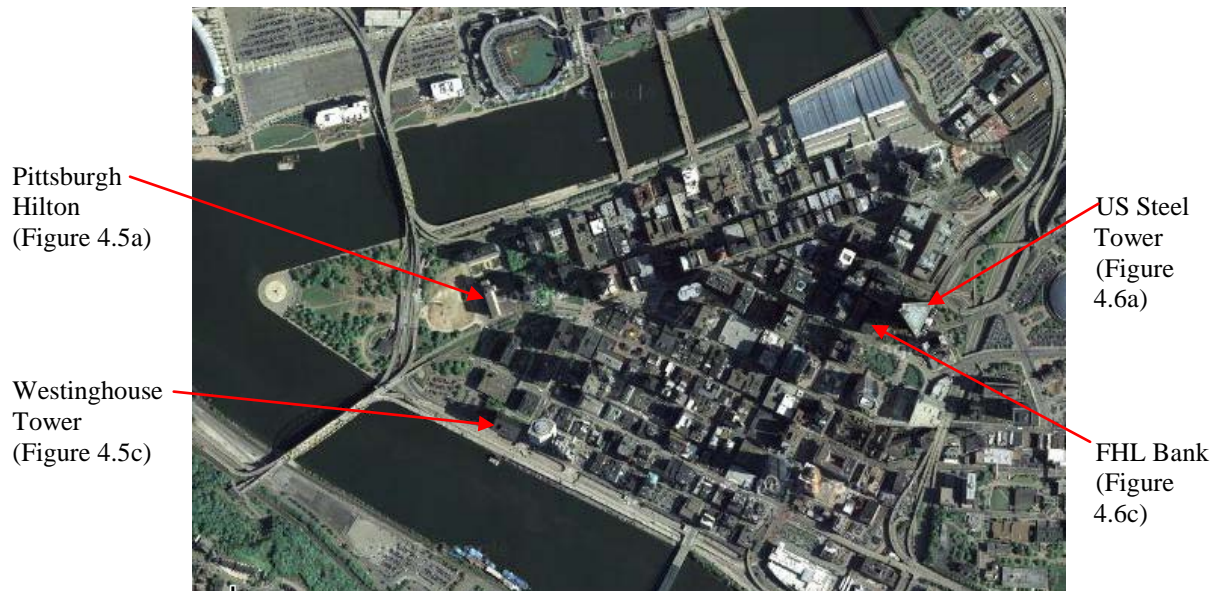


(a) Wind Rose



(b) Wind Speed (m/s) Distribution

Figure 4.3: Wind Characteristics for Pittsburgh, PA, 2005-2008



(a) Aerial View of downtown Pittsburgh, PA (Google Maps)

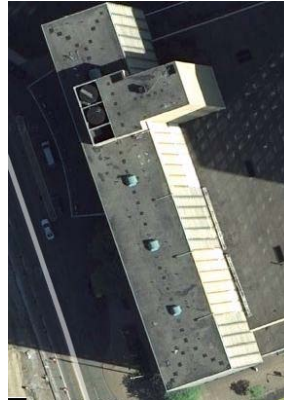


(b) 'West face' of Pittsburgh
(Pittsburgh Visitors and Convention Bureau)

Figure 4.4: Views of Pittsburgh, PA



(a) Pittsburgh Hilton and Towers (Glass, Steel, and Stone)



(b) Aerial view of Pittsburgh Hilton (Google Maps)



(c) Westinghouse Tower (Mark Moriarty)



(d) Aerial view of Westinghouse Tower (Google Maps)

Figure 4.5: Perimeter Buildings for Pittsburgh study



(a) U.S. Steel Tower (Glass, Steel, and Stone)



(b) Aerial view of tower (Google Maps)



(c) FHL Bank Building (Glass, Steel, and Stone)



(d) Aerial view of FHL (Google Maps)

Figure 4.6: Interior Buildings for Pittsburgh Study

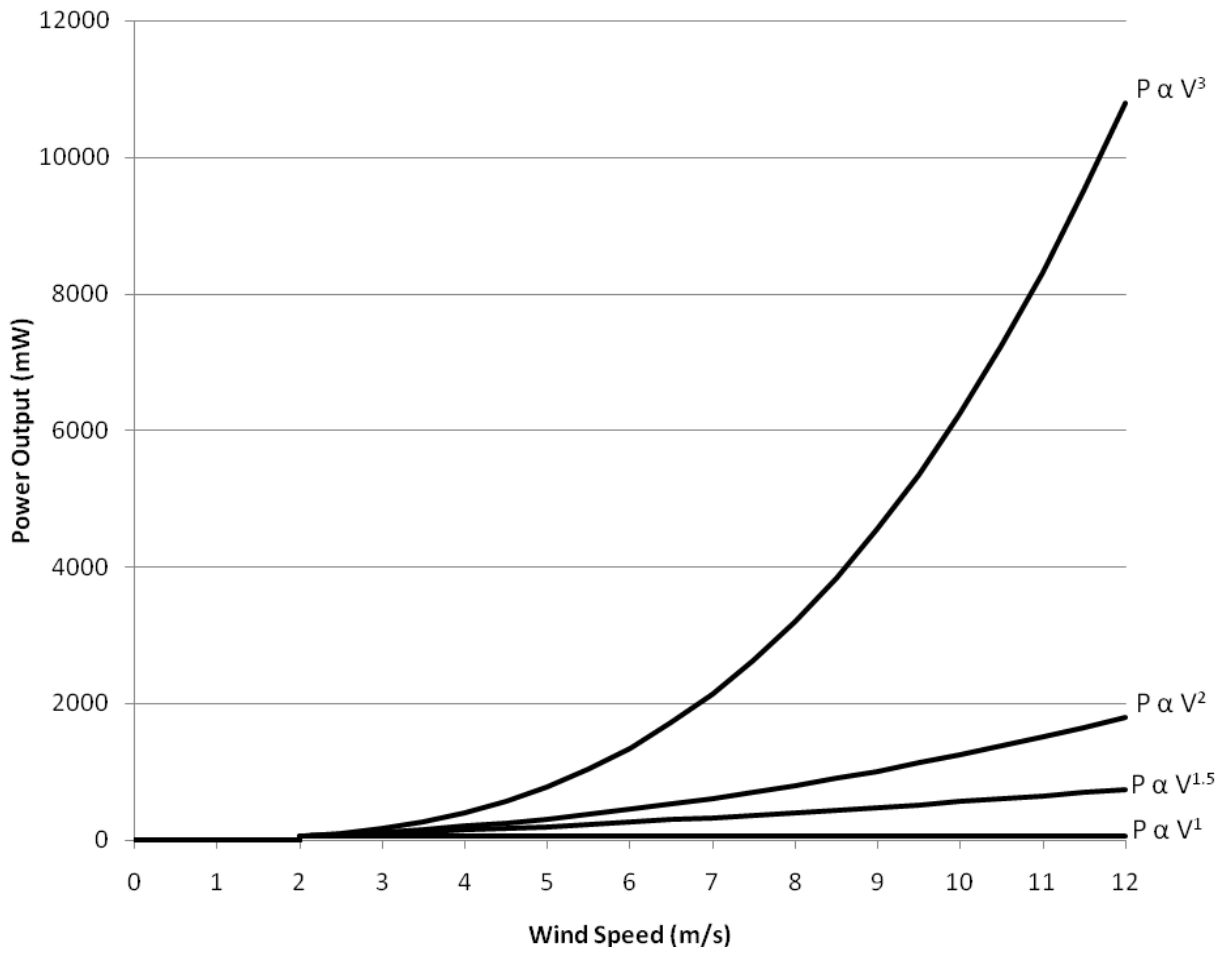
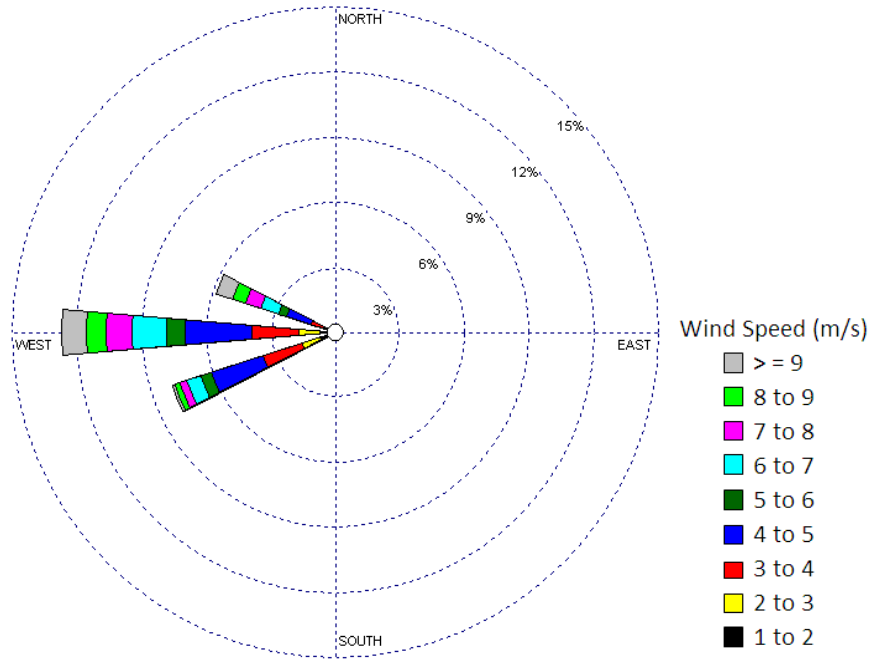
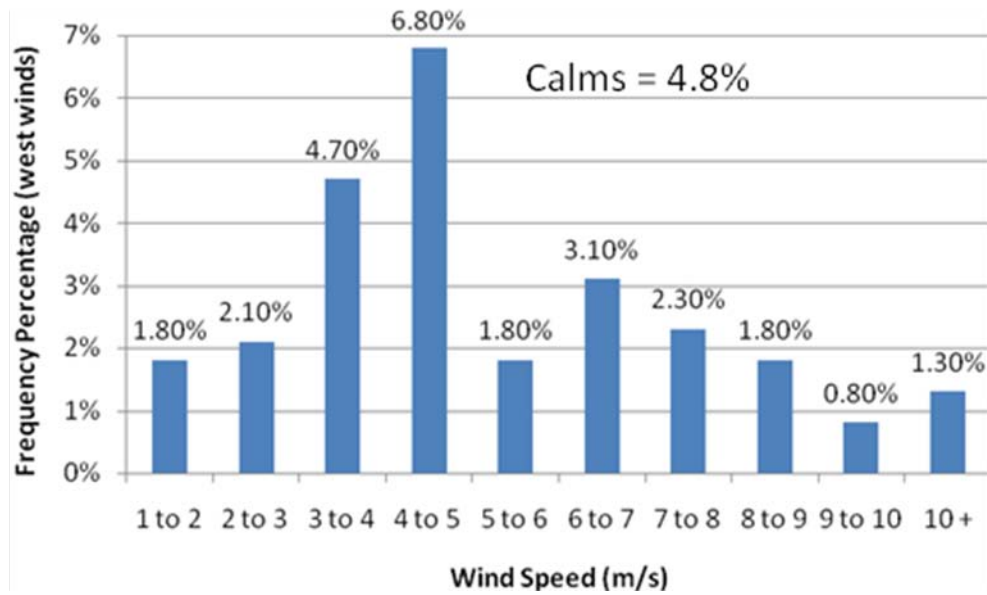


Figure 4.7: Potential AEH Power Curves



(a) Wind Rose



(b) Open field wind speed (m/s)

Figure 4.8: Wind Characteristics for AEH Operating Range 236° to 304° (WSW to WNW Segments)

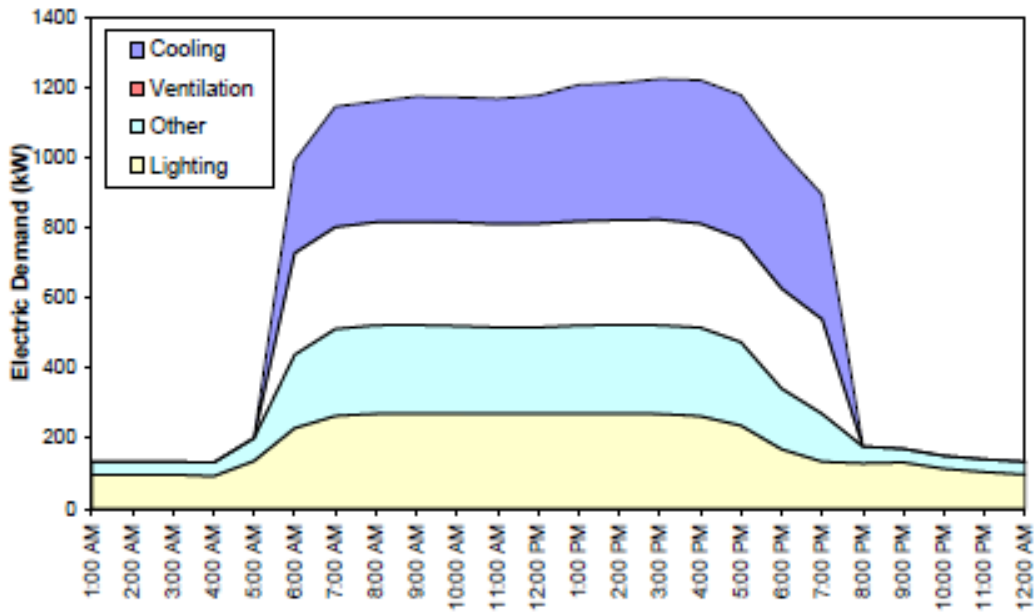


Figure 4.9: Hourly Electric loads for 250,000 ft² Chicago office building (US EPA)

5.0 CONCLUSIONS AND FUTURE RESEARCH DIRECTIONS

There were two primary objectives in this work. First, using LCA, the environmental impacts of an AEH were investigated, and alternative materials were investigated to reduce these impacts. The current version of the AEH was modeled. Alternative materials, such as 100% recycled aluminum, wood, and steel were substituted for individual parts of the AEH's frame and the environmental impacts were analyzed. Finally, a decision matrix was created to determine an 'optimized' version of the prototype AEH. Categories such as strength, energy consumption, and cost were used, the original materials were assigned a value of 1, and each alternative material was assigned a value based on their deviation from the original material in each category. Both energy and CO₂ payback periods were calculated based on outputs determined in Chapter 4, and compared to current photovoltaic and small-scale wind turbine studies.

Secondly, a method was proposed to determine the potential of wind energy generation in an urban setting. This method took data from a readily available source, an airport, and created a range of wind speeds at selected buildings in downtown Pittsburgh. The range of wind speeds were determined using current research on wind speed behavior, including roughness changes, building elevation, and concentrator effects. These wind speed results were applied to multiple assumed power curves for the AEH to determine a range of potential energy outputs. Specific conclusions are as follows:

1. The energy required to produce materials and manufacture the AEH is much higher than the amount of energy the AEH is calculated to produce, but an increase in output and decrease in required energy by one order of magnitude would prove the AEH is feasible in this sense.
2. 100% recycled aluminum requires much less energy to produce than virgin aluminum does, is approximately 1/3 the weight of steel, and is much stronger than wood, making it a strong option for AEH improvements.
3. The four steps described in this study provide a foundation for analyzing wind energy potential in an urban environment and are not specific to the AEH or Pittsburgh, PA and can be used with any wind energy generator in any urban location.
4. Average wind speeds are lower in a city setting than an open field setting. Wind speeds at the perimeter of the urban district will be faster than the speeds seen in the interior area.
5. Buildings that are significantly taller than the surrounding buildings should not experience a large reduction in wind speeds compared to the shorter buildings located in a city's interior. Shorter buildings located in the middle of a city experience the greatest wind speed reduction from the open field values. Also, the concentrator effect of the wind accelerating around the shorter roof level is minimized.
6. Application of AEHs in shorter interior buildings should focus on the creation of vortices along streets (wind canyon and channeling effects) that are running perpendicular to the predominant wind flow direction because the AEH operates more effectively in turbulent wind flow.

7. In Pittsburgh, PA, wind speeds are less than 5 m/s 65% of the time, thus increasing the need to strive for a low operating speed of the AEH and any other technology that may be developed for similar uses.
8. The AEH in its current state will not make a significant impact in a large office building's energy demands. While these results are still preliminary, they indicate the performance of AEH needs to improve by approximately an order of magnitude (which is possible) to make an impact in an urban district.

5.1 FUTURE RESEARCH DIRECTIONS

This study was aimed at performing an LCA on an AEH prototype and use LCA methods to explore alternative material options to reduce the environmental impact of producing the AEH. The second part of this study focused on creating a method to use readily available wind speed data from an open field (airport) location and transforming it into wind speeds at the roof levels of selected buildings inside a downtown district; Pittsburgh, PA was used in this case.

The results coming from the LCA highlighted the need to either increase the output of the AEH or reduce the energy requirements and other environmental impacts of production. Reducing energy consumption/environmental impacts and increasing output by roughly an order of magnitude should result in the AEH being viable for use. The energy payback time would be within the 20 year assumed lifetime and the environmental impacts per kWh produced would be comparable to other small-scale wind turbines and photovoltaics. As the AEH continues to improve, LCA can be used to update the energy requirements and/or impacts. Also, LCA allows

alternative materials to be explored to determine if they would be environmentally friendly options.

Chapter 4 of this study focused on required steps to take open field wind data and transform it into corresponding urban wind speeds. The power curves created represented a range of potential outputs of the AEH. As testing continues, a true power curve should be created to improve upon the accuracy of the AEH's energy output. This study relied heavily on previous studies focusing on wind flows in complex environments, which were completed both by wind tunnel testing or utilizing Computational Fluid Dynamics (CFD). CFD of wind flow has been shown to provide results similar to what truly happens in the environment. The approach reported in Chapter 4 could be used to a) exclude sites from further consideration; or b) provide guidance for a more focused site assessment or more complex CFD analysis. As production of the AEH continues, test buildings could be studied using CFD to determine the local wind environment and whether the AEH would be a viable option for alternative energy production.

Two more subjects that were not discussed in this study were the economics of the AEH as well as its potential for use in developing countries. Since the AEH is just a prototype, an economic analysis is not conducive at this stage as the design will constantly be updated with different materials, sizes, etc. This study only focused on use in a developed downtown district. However, while the AEH currently only produces a small amount of electricity, in the future, this technology may find a use in less industrialized nations, providing enough energy to power a small number of laptops in a computer lab or similar applications. As the energy output of the AEH increases, the application may shift from small items such as wireless sensors in buildings to providing a small percentage of the minimum constant electric demand of an office building or hotel.

BIBLIOGRAPHY

- Aerovironment. Architectural Wind™ AVX 1000. <http://www.avinc.com/>. 2009
- Allen, S. R., G. P. Hammond, M. C. McManus, 2008. "Energy Analysis and Environmental Life Cycle Assessment of a Micro-wind Turbine." Proceedings of the Institution of Mechanical Engineers, Part A: Journal of Power and Energy 222.7: 669-684.
- American Society of Civil Engineers. ASCE 7 – 05: Minimum Design Loads for Buildings and Other Structures v. 7-05. Structural Engineering Institute. 2006.
- Bagatti, Tim, Personal Correspondence, June 2009.
- Baumann, H, and A.M. Tillman. The Hitch Hiker's Guide to LCA. Lund, Sweden: Studentlitteratur AB, 2004. p. 97.
- Coccal, O., A. Dobre, T.G. Thomas, S. E. Belcher, 2007. "Structure of Turbulent Flow Over Regular Arrays of Cubical Roughness." Journal of Fluid Mechanics 589.1: 375-409.
- Coccal, O., T. G. Thomas, I.P. Castro, S. E. Belcher, 2006. "Mean Flow and Turbulence Statistics over Groups of Urban-like Cubical Obstacles." Boundary-Layer Meteorology 121.3: 491-519.
- Coccal, O. and S. Belcher, 2005. "Mean Winds through an Inhomogeneous Urban Canopy." Boundary-Layer Meteorology 115.1: 47-68.
- Coccal, O. and S. E. Belcher, 2004. "A Canopy Model of Mean Winds Through Urban Areas." Quarterly Journal of the Royal Meteorological Society 130.599: 1349-1372.
- Cole, D. and L. M. Weiland. 2009, "An Analysis of Micro Aeroelastic Energy Harvesting Devices." Proceedings of Dynamic Systems and Control Conference 2009.
- Davenport, A.G., 1965. "The Relationship of Wind Structure to Wind Loading." Proceedings of the Symposium on Wind Effects on Buildings and Structures. Vol. 1. National Physical Laboratory. Teddington. U.K., Her Majesty's Stationery Office. London: 53-102
- Dayan, E., 2006 "Wind Energy in Buildings: Power Generation from Wind in the Urban Environment - where it is needed most." Refocus 7.2: 33-38.

- Energy Information Administration, Electric Power Monthly: April 2009. Report No.: DOE/EIA-0226
- Energy Information Administration. Annual Energy Review, 2007.
- Energy Information Administration. 2003 Commercial Buildings Energy Consumption Survey. 2006.
- Fava J, R. Denison, B. Jones, M.A. Curran, B. Vigon, S. Selke, J. Barnum, 1991. "A Technical Framework for Life-Cycle Assessment." SETAC. 155.
- Grimmond, C. S. B. and T. R. Oke, 1999. "Aerodynamic Properties of Urban Areas Derived from Analysis of Surface Form." Journal of Applied Meteorology 38.9: 1262.
- Global Wind Energy Council (GWEC). Global Wind 2008 Report.
- Hondo, H., 2005. "Life cycle GHG Emission Analysis of Power Generation Systems: Japanese case." Energy 30.11-12: 2042-2056.
- Humdinger Wind Energy LLC. Windbelt™ Generator. <http://www.humdingerwind.com/>. 2009.
- International Aluminum Institute. "Life Cycle Inventory of the Worldwide Aluminum Industry with Regard to Energy Consumption and Emissions of Greenhouse Gases." March 2003. IAI, London. www.world-aluminium.org
- ISO 14040, 1998. "Environmental Management – Life Cycle Assessment – Principles and Framework." Geneva, Switzerland: International Standard Organization.
- Kim, K. C., H. S. Ji, S. H. Seong, 2003. "Flow Structure round a 3-D Rectangular Prism in a Turbulent Boundary Layer." Journal of Wind Engineering and Industrial Aerodynamics 91.5: 653-669.
- Kastner-Klein, P. and M. W. Rotach, 2004. "Mean Flow and Turbulence Characteristics in an Urban Roughness Sublayer." Boundary-Layer Meteorology 111.1: 55-84.
- Lakes Environmental. "WRPLOT View – Wind Rose Plots for Meteorological Data." <http://www.weblakes.com/lakewrpl.html>. 2009.
- Lenzen, M. and J. Munksgaard, 2002. "Energy and CO2 Life Cycle Analysis of Wind Turbines- Reviews and Applications." Renewable Energy 26: 339–362.
- Lu, L. and K. Y. Ip, 2009. "Investigation on the feasibility and enhancement methods of wind power utilization in high-rise buildings of Hong Kong." Renewable and Sustainable Energy Reviews 13.2: 450-461.
- Martínez, E., F. Sanz, S. Pellegrini, E. Jiminez, J. Blanco, 2009. "Life Cycle Assessment of a Multi-Megawatt Wind Turbine." Renewable Energy 34.3: 667-673.

- Mertens, S., 2002. "Wind Energy in Urban Areas : Concentrator Effects for Wind Turbines Close to Buildings." Refocus 3.2: 22-24.
- Mertens, S., 2003. "The Energy Yield of Roof Mounted Turbines." Wind Engineering 27.6: 507-518.
- National Climatic Data Center, 2003. "Quality Controlled Local Climatological Data" (v1.4). <http://cdo.ncdc.noaa.gov/qclcd/QCLCD?prior=N>
- Oke, T. R., 1988. "Boundary Layer Climates." Routledge.
- Peacock, A. D., D. Jenkins, M. Ahadzi, A. Berry, S. Turan, 2008. "Micro Wind Turbines in the UK Domestic Sector." Energy and Buildings 40.7: 1324-1333.
- Pre Consultants. SimaPro Life Cycle Assessment software [v7.1], 2007 (The Netherlands, Amersfoort).
- Rankine, R., J. Chick, G. P. Harrison, 2006. "Energy and Carbon Audit of a Rooftop Wind Turbine." Proceedings of the Institution of Mechanical Engineers, Part A: Journal of Power and Energy 220.7: 643-654.
- Ricciardelli, F. and S. Polimeno, 2006. "Some Characteristics of the Wind Flow in the Lower Urban Boundary Layer." Journal of Wind Engineering and Industrial Aerodynamics 94.11: 815-832.
- Richards, P. J. and R. P. Hoxey, 2008. "Wind Loads on the Roof of a 6 m Cube." Journal of Wind Engineering and Industrial Aerodynamics 96.6-7: 984-993.
- Simiu, E., and R.H. Scanlan, 1986. "Wind Effects on Structures: 2nd Edition", John Wiley & Sons, Inc., New York.
- Skote, M., M. Sandberg, U. Westerburg, L. Claesson, A.V. Johansson, 2005. "Numerical and Experimental Studies of Wind Environment in an Urban Morphology." Atmospheric Environment 39.33: 6147-6158.
- Stathopoulos, T., P. Saathoff, X. Du, 2002. "Wind Loads on Parapets." Journal of Wind Engineering and Industrial Aerodynamics 90.4-5: 503-514.
- Swift. Swift Rooftop Wind Energy System™. <http://www.swiftwindturbine.com/?intro=skip>. 2009.
- US Department of Energy, "Wind Resource Maps". Accessed May 5, 2009. http://www.windpoweringamerica.gov/wind_maps.asp.
- US Department of Energy. "How Wind Turbines Work." Accessed May 5, 2009. http://www1.eere.energy.gov/windandhydro/wind_how.html#inside.

US Environmental Protection Agency. "Tool for the Reduction and Assessment of Chemical and other Environmental Impacts". <http://www.epa.gov/nrmrl/std/sab/traci/> Accessed July 9, 2009

US Environmental Protection Agency. "Office Building Energy Use Profile." EPA National Action Plan for Energy Efficiency.

Weisser, D., 2007. "A Guide to Life-Cycle Greenhouse Gas (GHG) Emissions from Electric Supply Technologies." Energy 32.9: 1543-1559.

Yingni, J., 2006. "Wind Power Density Statistics Using the Weibull Model for Inner Mongolia, China." Wind Engineering 30.2: 161-168.